"Man can learn nothing except by going from the known to the unknown".

***Claude Bernard** (1813–1878), French physiologist.*
An Introduction to the Study of Experimental Medicine.

CHAPTER 4

RAW MATERIALS CHARACTERISATION

4.1 INTRODUCTION.

This chapter is mainly concerned with the characterisation of the three PANIPOL^{TM} complexes. A general account on the details of the techniques employed is presented followed by the results following from them. Some of these techniques, as will be seen in due course, were also used in the characterisation of the blends and extrudates. These will be revisited in the relevant chapters.

Great effort was put in the characterisation of the PANIPOL^{TM} complexes as it was important to have a more detailed information on their inherent restrictions, especially those related with their thermal processing. In respect of this, it is true that information was provided by the supplier. However, as will be seen later, and as indicated by Neste Oy Chemicals, differences in the samples thermal behaviour and stability were found. Moreover, it was found that their rheology was also different. Therefore, it was needed to find those distinctive characteristics that, eventually, would aid in selecting the more suitable sample to be blended with the polymer matrices with the final purpose of in-situ forming the PANI into fibres. At the same time, through these analyses it was possible to establish the basis for selecting the processing conditions and the polymer matrix, under those conditions, more likely to promote the in-situ formation of the fibres.

It was also important to understand the chemistry of the samples' components. Regarding this, the analysis was centred on only one selected sample (PANIPOL^{TM} 2) because, as informed by the company supplying the material, the basic chemistry was the same in all the samples. Taking this into account it was assumed that the morphology of the samples would be also similar and only PANIPOL^{TM} 2 was analysed. It was assumed that the same would apply to the conductivity level of the samples and, for this matter; the analysis was performed only on the same sample. Despite the fact that information was provided on the subject, it was needed to corroborate this. As will be seen, PANIPOL^{TM} 2 was the sample more suitable to be deformed into fibres, which justified that the analyses were mainly concentrated on this. It was felt that knowing about the chemistry of the samples was important, as this would be correlated with their morphology, which in turn would aid in the interpretation of the morphology observed in the extrudates. This will be dealt with in the relevant chapter.

Finally, it was also interesting to obtain structural information on the PANIPOL™ complexes. For this, X-ray diffraction experiments were conducted with the three samples. This analysis also provided information about the samples' composition.

4.2 X-RAY DIFFRACTION.

Wide angle X-ray diffraction experiments were carried out to obtain structural information on the three PANIPOL™ samples. The experiments were performed with a Philips 1050 Goniometer X-ray diffractometer. The essential features of a diffractometer are shown in figure 4.1. X-rays from the tube T are incident on the sample S, which may be set at any desired angle *(θ)* to the incident beam by rotation around an axis through O, the centre of the diffractometer circle. D is a counter, which measures the intensity of the diffracted X-rays. This can also be rotated around O and set at any desired angular position *(2θ).*

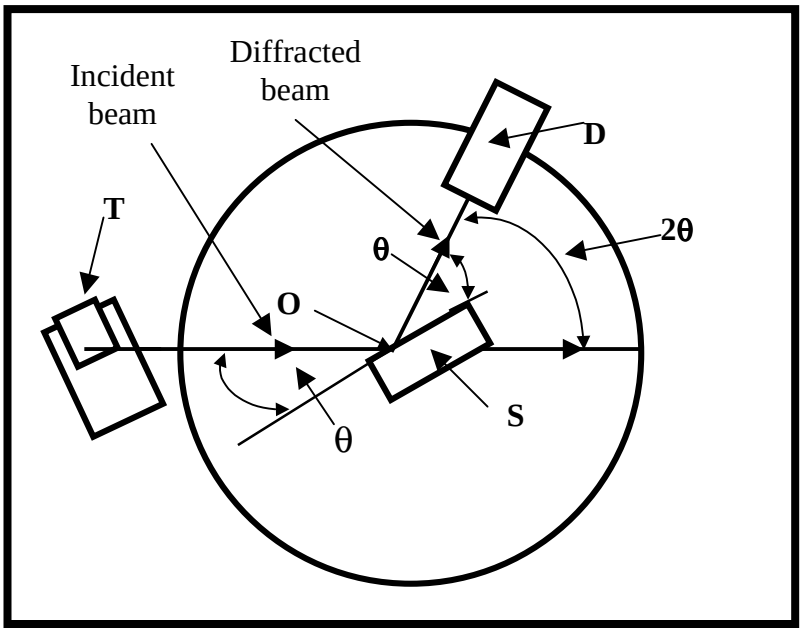

Figure 4.1. Diagram showing the essential features of a diffractometer.

During the experiments, an X-ray beam of constant wavelength *(λ)* was incident on the sample. This resulted in the diffraction of the beam by the atomic planes in the sample. The intensity of the diffracted beam was then measured by the instrument counter at different 2*θ* positions, and the spacing distances *(d')* between the parallel

planes in the sample were calculated in accordance with the Bragg law [159] equation (*Eq. 4.1*).

$$n\lambda = 2d' \sin\theta \text{ .....} Eq.\ 4.1.$$

In equation 4.1, n is called the diffraction order and in practice is considered to be of first order with a given value equal to 1. The experiments, data collection and numerical calculations were performed using an advanced X-ray diffraction scan processing software (Traces for Windows^{TM}, version 3.0). During the experiments, nickel-filtered copper-$K\alpha$ radiation, with a wavelength of 1.5406 Å, was used. The diffractometer was operated at 36 kV and 26 mA.

For the experiments, a few of the as-received PANIPOL^{TM} pellets were powdered with a pestle and mortar. The diffraction pattern was then obtained by scanning the powder in an interval of 2θ = 6 to 80 degrees at a rate of 0.02 degree/s. Experiments were also carried out on the pyrolysed pellets. About 25 g of the pellets were placed in a crucible and the pyrolysis was performed in a Lenton furnace (Serial No. 4904) at 850°C for 2 hrs. Afterwards the crucible containing the pyrolysis product was cooled down in a desiccator where it was kept until it was ready for further analysis. The analysis was performed in the same diffractometer using the experimental conditions above described.

The X-ray diffraction pattern of the powdered pellets of PANIPOL^{TM} is presented in figures 4.2 and 4.3. Figure 4.2 shows the diffraction pattern of samples 1 and 2 while fig. 4.3 corresponds to that of sample 3. As can be observed, the level of crystallinity detected in the three samples is relatively low. However, the diffraction patterns are different, especially the one corresponding to the sample 3. The difference in the diffractograms suggests some differences in the composition of the samples. From the reflections presented in the figures only a few can be clearly associated with crystalline regions. The angles at which these occurred and their respective d'-spacing are presented in Table 4.1.

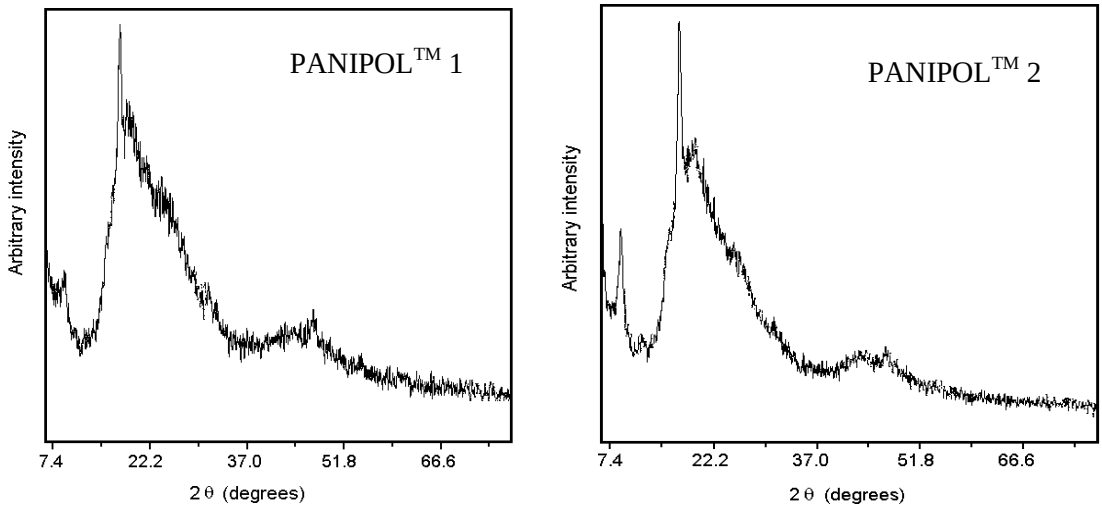

Figure 4.2. X-ray diffraction pattern of the powdered PANIPOL™ pellets.

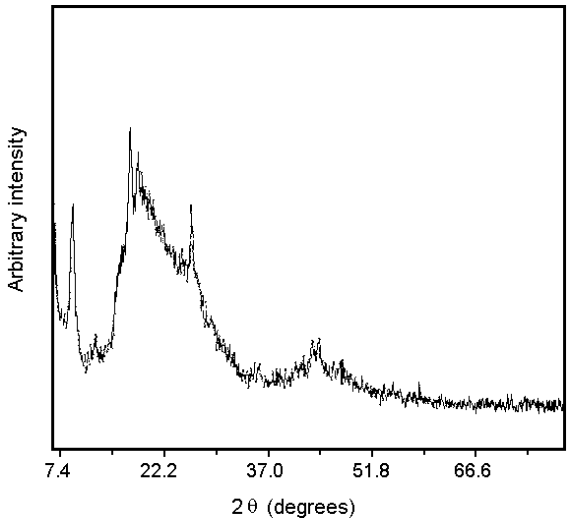

Figure 4.3. X-ray diffraction pattern of the powdered pellets of PANIPOL™ 3.

Table 4.1. Main reflections found in the scan of the PANIPOL™ powder.

PANIPOL™ 1	
2θ angle (degrees)	**d'-spacing (Å)**
9	9.64
17	5.09
47	1.93
PANIPOL™ 2	
2θ angle (degrees)	**d'-spacing (Å)**
9	9.86
18	5.07
47	1.94

Table 4.1 (Continued).

PANIPOL™ 3	
2θ angle (degrees)	**d'-spacing (Å)**
9	9.59
17	5.09
19	4.78
26	3.42
44	2.05
48	1.91

The X-ray diffractograms of a yellow powder collected from each of the pyrolysis products of the three PANIPOL™ samples were identical. A selected diffractogram is presented in figure 4.4. From this, it can be observed that the reflection peaks obtained during the scanning of the sample are very well defined, which indicates a relatively high level of crystallinity. Table 4.2 presents the angles at which the main reflections occurred, and their respective relative intensities and d'-spacing.

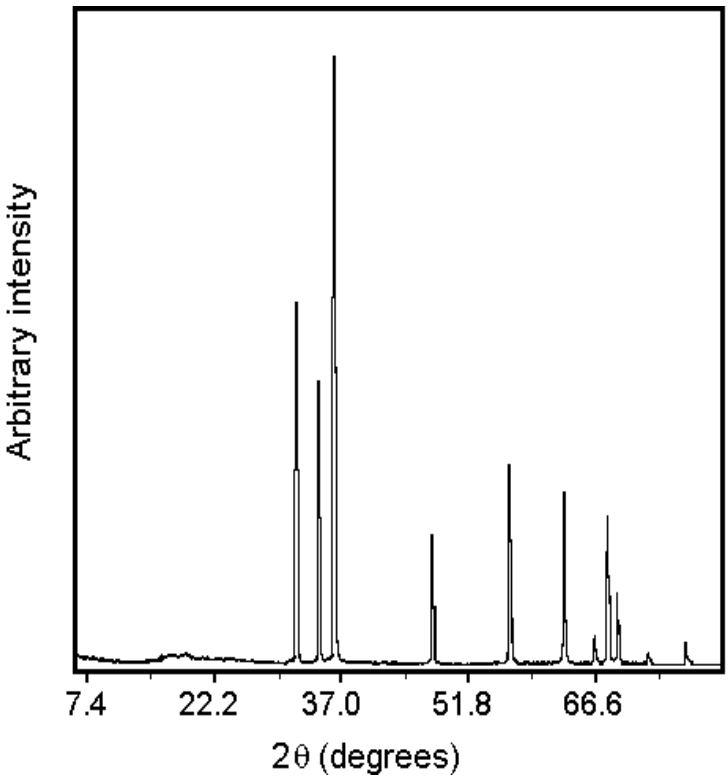

Figure 4.4. X-ray diffraction pattern of the yellow powder found in the three pyrolysed PANIPOL™ samples.

Table 4.2. Main reflections found in the scan of the yellow powder found in the three pyrolysed PANIPOL™ samples.

2θ angle (degrees)	**Relative intensity**	**d'-spacing (Å)**
32.02	59	2.793
34.69	42	2.584
36.49	100	2.460
47.79	21	1.902
56.78	32	1.620
63.06	28	1.473
66.56	4	1.404
68.14	24	1.375
69.27	12	1.355
72.76	2	1.299
77.11	3	1.236

The relative intensities presented in Table 4.2 together with their corresponding d'-spacing, are in good agreement with those reported for zinc oxide (ZnO) [160]. It is possible that the presence of ZnO in the pyrolysis product of the PANIPOL™ pellets is the result of the reaction between the element zinc (Zn) (a decomposition product of the pellets during the pyrolysis) and atmospheric oxygen. Therefore, these results initially confirm the presence of this element in the pellets, originally forming part of the zinc compound.

4.3 GRAVIMETRIC ANALYSIS.

This analysis was performed in order to confirm the amount of the conducting polyaniline salt (emeraldine salt, ES) in the as-received pellets of PANIPOL™. Through this analysis, additional information was also sought on the amount of doping agent used for the production of the ES. Also, as it will be seen, the analysis provided a first insight on the identity of the doping agent used.

In general terms, a gravimetric analysis is based on a technique in which the constituent searched for is separated from the original sample and weighed [161]. The desired constituent is usually isolated or separated by precipitation, and the percentage of this is calculated from the weights of the original sample and precipitate.

Accordingly, the ES was separated from the PANIPOL^{TM} pellets by dissolving these in acetone. This chemical was used because does not dissolve the ES [65]. This, in principle, would allow the precipitation and separation of the ES from the rest of the sample. In a similar manner, an ammonium hydroxide solution (NH_4OH) was used to extract the doping agent from the ES. NH_4OH was used because is a well-known [20,21,67,150,162,163] effective extracting agent. Consequently, assuming that pure ES is the sample reacting with NH_4OH, this in theory would give an indication about the amount of doping agent used. The details about the experiments are described in the following sections.

4.3.1 SEPARATION OF THE POLYANILINE SALT FROM THE PANIPOL^{TM} COMPLEX.

This process was accomplished by dissolution of the pellets in acetone (C_3H_6O, 99 % purity, from Aldrich) by using a Kerry's LTD ultrasonic bath. PANIPOL^{TM} 2 was selected for the analysis. A few pellets of the sample (about 12 g) were pulverised with a pestle and mortar. Four suspensions of the powdered pellets in an excess of acetone, contained in previously dry-weighed test tubes, were sonicated for 15 min. Afterwards they were centrifuged for 15 min at 3000 rpm in a MSE centrifuge (Serial No. 0-5201.A). The solutions in the test tubes were decanted and a sample was collected for further examination. An excess of clean acetone was further added to the remaining sediments (or precipitates) in the bottom of the test tubes, and the suspensions so obtained were subjected to the same sonication, centrifugation and decanting processes. This was carried out several times until the decanted solution was clean and transparent. After the conclusion of seven dissolution cycles, the test tubes with their respective remaining sediments were placed in a Gallenkamp vacuum oven at 40°C where they were kept overnight to evaporate any possible remains of acetone. Subsequently, they were taken to a desiccator where they were kept until ready for further examination. The test tubes with their respective remaining sediments were weighed and the weight percent of the sediments in each sample was calculated. Before starting the experiments, the empty test tubes were dried overnight in an oven at 40°C to be further weighed. Samples of about 2 g of the powdered pellets were used. About 12 ml of acetone was used in each cycle.

The solutions decanted from each of the dissolution cycles showed an initial opaque brownish colour. The opacity and the colour intensity of the solutions decreased as the number of dissolution cycles was increased. The samples collected from the last cycles were transparent and uncoloured. This suggested that the process of dissolution in acetone of any additives susceptible to dissolution, and originally present in the sample had been completed. It was noticed that after a few minutes of being collected, the decanted solutions from the first dissolution cycles also showed a whitish precipitated solid. This colour is reported by Kärnä et al. [164,165] as characteristic of the reaction product of the mixture of ZnO with dodecylbenzene sulphonic acid (DBSA). Therefore it is believed that the precipitate may be a Zn salt of DBSA, that is, $Zn(DBS)_2$ (the zinc compound, Zn dodecylbenzene sulphonate). It was also noticed that these solutions became frothy when they were put in contact with water. This is a characteristic of surfactants, for example DBSA, or its derived salts [166,167]. Therefore, it is believed that the solutions decanted may consist of a solution of Zn and DBS ions in acetone. It was also noticed that the colour of the sediment obtained after the completion of the dissolution cycles, did not change with respect to the colour of the original powdered PANIPOL™ samples. This presented a dark-green colour, characteristic of the ES (doped polyaniline) [20,21,67,150,162,163].

The remaining sediment weight percent (*sed.wt.%*) in each of the samples previously subjected to the seven dissolution cycles in acetone was calculated using the following *equation*:

$$sed.wt.\% = \frac{w_F - w_T}{w_I - w_T} x100 = \frac{w_S}{w_P} x100 \text{ .....} Eq.\ 4.2,$$

where:

w_F = final weight of dry test tube + dry sediment,

w_T = weight of empty dry test tube,

w_I = initial weight of dry test tube + powdered PANIPOL™ 2,

w_S = final weight of dry sediment, and

w_P = initial weight of powdered PANIPOL™ 2.

The values of the terms defined in *Eq. 4.2* and the results from the calculations are presented in Table 4.3.

Table 4.3. Values of the terms in *Eq. 4.2* and the calculated sediment weight %.

Sample	w_T (g)	w_I (g)	w_F (g)	w_P (g)	w_S (g)	*wt.%*
1	7.111	9.111	7.659	2.000	0.548	27.40
2	7.146	8.825	7.538	1.679	0.392	23.35
3	9.680	11.862	10.174	2.182	0.494	22.64
4	9.671	11.948	10.214	2.277	0.543	23.85
Sediment average *wt.* % = 24.31						

As doped polyaniline does not dissolve in acetone, then it is believed that the average wt. % of 24.31 corresponds to the weight percent composition of the ES in the original powdered samples of PANIPOL^{TM} 2 pellets. On the other hand, the weight loss, that is, the 75.69 %, mainly corresponds to $Zn(DBS)_2$. As the powdered pellets were not previously dried for the analysis, then it is possible that the above indicated weight % loss also counts for some residual water initially absorbed from the environment as a result of the hygroscopic nature of the DBS salt. These results are in good agreement with the information provided by the supplier regarding a content of approximately 25 % of polyaniline salt (ES) and 75 % of a Zn compound in the pellets. The diagram presented in figure 4.5 summarises the sequence of the separation process.

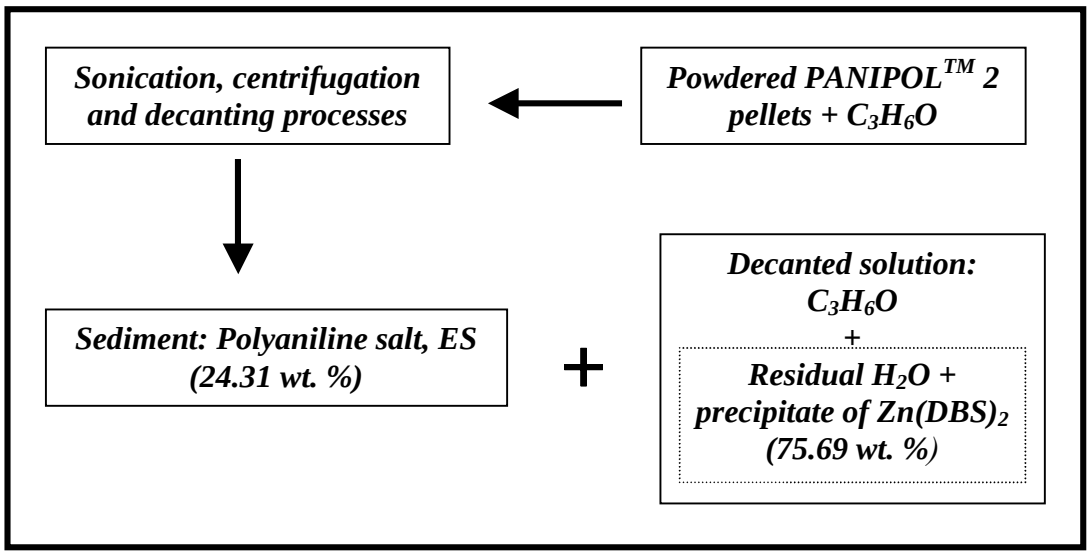

Figure 4.5. Diagram summarising the separation process of the ES from powdered pellets of PANIPOL^{TM} 2.

4.3.2 EXTRACTION OF THE DOPING AGENT FROM THE POLYANILINE SALT.

A similar process to the one described in the previous section was performed. A solution of NH_4OH was prepared to react with the sediment yielded from one of the powdered PANIPOL^{TM} 2 samples previously dissolved in acetone (sample No. 1 from the previous section and referred to in this section as the ES). For this, a ca. 10 vol. % ammonia aqueous solution was prepared by dissolving 1.0 vol. part of ammonia (NH_3, 35 wt. %, 0.880 specific gravity, from BDH Laboratory) in 3.5 vol. parts of distilled water. The NH_4OH was added in excess to the ES and after sonication for 15 min, the suspension in the test tube was left to rest overnight in order to complete the extraction of the doping acid by the NH_4OH. Afterwards it was centrifuged for 15 min at 3000 rpm. The solution in the test tube was decanted and, to eliminate any excess of dopant possibly left, an excess of acetone was added to the remaining sediment. The suspension so formed was sonicated for 15 min and afterwards it was left to rest overnight in the test tube. Subsequently, the suspension was centrifuged for 15 min at 3000 rpm and the solution in the test tube was decanted. Distilled water was added to the remaining sediment and the suspension so obtained was subjected to the same sonication, centrifugation and decanting processes previously described. The test tube with the remaining sediment was taken to the vacuum oven where it was kept overnight at 40°C to evaporate any remaining water. Finally, the sediment in the test tube was kept in a desiccator until it was ready for further weight percent calculation. About 15 ml of NH_4OH and acetone were respectively used in the experiments.

After subjecting the ES-NH_4OH suspension to the sonication and further centrifugation processes, a purplish-blue solution was decanted that presented a frothy appearance. As has been mentioned before, DBSA and its derived salts also present that frothy appearance. On the other hand, it is known that DBSA and its derived salts are also used for doping polyaniline [66,71]. Therefore, these facts suggested the possibly presence of the DBSA in the decanted solution as a result of this being extracted by the NH_4OH from the ES. This observation indicates that DBSA was possibly used for doping the polyaniline. Furthermore, it was also noticed that the sediment deposited in the bottom of the test tube showed a violet-bluish colour, which is expected [48,67] for undoped polyaniline (emeraldine base, EB, the non conducting form of polyaniline).

Moreover, it has also been reported [20,21,67,150,162,163] that this bluish powder is obtained when the ES complex is put in contact with ammonia solutions, and what is more, the ammonia solutions become frothy with the extracted acid during de-doping process. Therefore, this strongly suggested that the sediment yielded mainly consisted of EB. It was additionally observed that after adding an excess of acetone to the remaining sediment, the solution decanted after further sonication and centrifugation of this suspension, also looked like a detergent, especially when it was mixed with water. Again, this may be due to the surfactant property of the DBSA forming a solution with acetone and that was not completely extracted from the sediment by the NH_4OH. After washing the remaining sediment with distilled water, following the already mentioned sonication and centrifugation processes, the decanted solution still looked frothy which suggested that some of the doping agent still remained unextracted from the ES. The final sediment weight percent (*f.sed.wt.*%), with respect to the initial sediment weight, w_S, (from Table 4.3), was calculated using the following equation:

$$f.sed.wt.\% = \frac{w_{F'} - w_T}{w_{S1}} x100 = \frac{w_{S2}}{w_{S1}} x100 \text{.....} Eq.\ 4.3,$$

where:

$w_{F'}$ = final weight of dry test tube + dry sediment = 7.390 g,

w_T = weight of empty dry test tube = 7.111 g (from Table 4.3),

w_{S1} = initial weight of dry sediment = 0.548 g (w_S from Table 4.3), and

w_{S2} = final weight of dry sediment = 0.279 g.

The calculated final sediment weight percent was 50.91. This suggests a wt. % loss of 49.09 in w_{S1}. Assuming that the final sediment is EB and that the weight percent loss corresponds to the extracted DBSA, then these results should in principle give an estimate of the EB:DBSA weight ratio. This is based on the fact that a minimum weight ratio of doping agent to EB should be observed in order to obtain a fully protonated doped complex, being this ratio of stoichiometric character and strictly depending on the type of doping agent used. Accordingly, the weight percentages above indicated give a EB:DBSA weight ratio of 1:0.96. However, this ratio should be different considering that the extraction of the doping agent from the EB was not complete. This is emphasised by Kärnä and co-workers [164] who suggest EB:DBSA weight ratios in

the range of 1:2.0 to 1:8.0 for the formation of EB-DBSA complexes with levels of conductivity in the range of 10^{-6} to 1.0 S/cm. Moreover, Levon et al. [72] suggest a EB:DBSA weight ratio of about 1:2.5 needed to obtain the correct stoichiometric proportion for the formation of the EB-DBSA complex.

As may be noticed, this analysis was not entirely conclusive about the nature and amount of the doping agent present in the pellets of PANIPOL^{TM}. Nevertheless, an initial hypothesis regarding the subject was established. The following section will provide additional assistance in the verification of the identity of the doping agent.

4.4 INFRARED SPECTROSCOPY.

Fourier transform infrared (FTIR) spectroscopy experiments were performed on the three as-received samples of PANIPOL^{TM}. Similarly, the same analysis was applied to the samples collected from the decanted solutions that were obtained from each of the seven dissolution cycles of the pellets of PANIPOL^{TM} 2 in acetone (refer to section 4.3.1). The analysed samples are identified as solutions 1 to 7, where solution 1 is the sample collected after the first dissolution cycle, and solution 7 the sample collected after the last cycle.

These experiments were performed to obtain information about the chemical structure of the main functional groups present in the samples so that in conjunction with the results from the previously described analytical methods, make possible the identification of the type of compounds initially present. This is possible based on the fact that the chemical bonds within the molecules of different organic and inorganic compounds absorb infra red (IR) radiation at specific wave number intervals or bands [168]. The absorption bands may be mainly considered as having two origins, these being the fundamental vibrations of functional groups, and skeletal groups (i.e. the molecular backbone or skeleton of the molecule), respectively. Absorption bands may also be considered as arising from stretching vibrations (i.e. vibrations involving bond-length changes), or deforming vibrations (i.e. vibrations involving bond-angle changes of the group). Each of these may, in some cases, be considered as arising from symmetric or asymmetric vibrations. The FTIR absorption spectrum is thus a "fingerprint" for a particular molecule that can be compared with reference spectra of

known compounds, thereby aiding in the identification of unknown samples and providing unambiguous confirmation of the identity of "known" materials.

The FTIR spectrum of the PANIPOL™ samples and solutions 1 to 7 was measured at room temperature with a Nicolet 710 FT-IR spectrometer in a spectral range of 4000 to 400 cm^{-1}. The PANIPOL™ specimens were prepared by grinding the powered pellets with potassium bromide (KBr) powder and then pressing the mixture into a tablet. The pulverisation of the pellets and mixture with KBr where respectively carried out with a pestle and mortar. The solutions were analysed by placing them, with the help of disposable micropipettes, between already prepared KBr discs.

It was found that the three PANIPOL™ samples presented a very similar FTIR spectrum. For simplicity, only a selected spectrum (PANIPOL™ 2) is presented in fig. 4.6. The assignments of the intensities of the main absorption peaks are shown in Table 4.4.

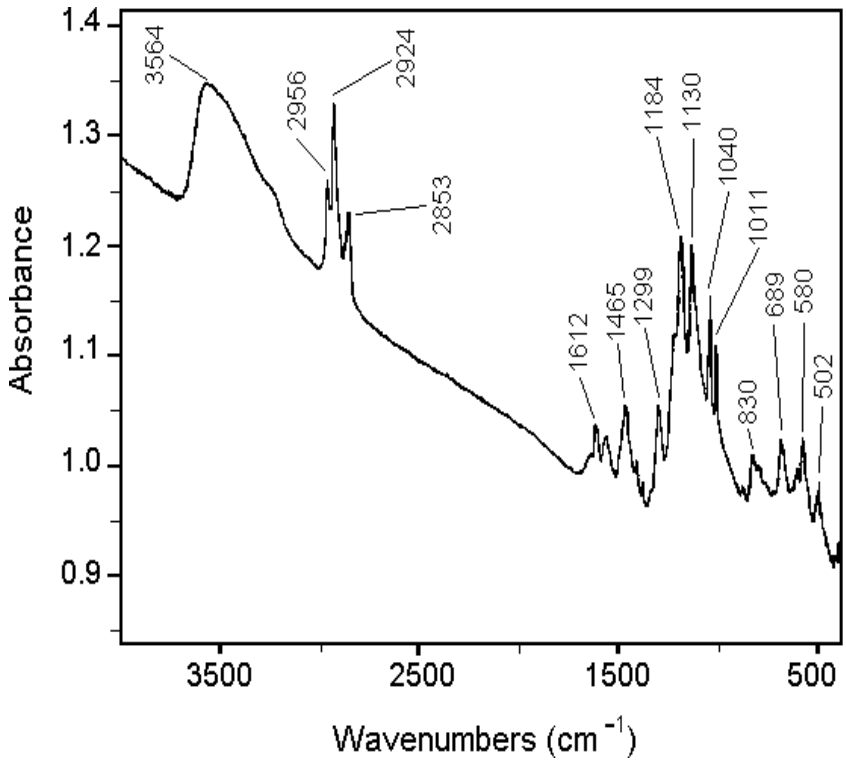

Figure 4.6. The FTIR spectrum of PANIPOL™.

Table 4.4. Assignments of the intensities of the main absorption peaks in the FTIR spectrum of PANIPOL™.

Absorption wave number (cm^{-1})	**Assignment**	**Comments**
3564	Hydroxyl group (OH).	Characteristic broad band in the interval 3600–3100 cm^{-1} [169].
2956	Carbon-hydrogen bond (C-H) asymmetric stretching vibration in the methyl group ($-CH_3$).	Medium to strong intensity characteristic band occurring at 2975-2950 cm^{-1} [169,170].
2924	C-H asymmetric stretching vibration in the methylene group ($-CH_2-$).	Medium to strong band intensity occurring at 2940-2915 cm^{-1} [169,170].
2853	C-H symmetric stretching vibration in $-CH_2-$.	Medium intensity band occurring at 2870–2840 cm^{-1} [169,170].
1612	Two possibilities: 1. Nitrogen-hydrogen bond (N-H) deformation vibration. 2. Carbon-carbon double bond (C=C) stretching vibration in aromatic ring.	1. Type of vibration (scissoring) normally occurring in primary aromatic amines at 1615-1580 cm^{-1} [169,170]. 2. Occurring at 1625–1590 cm^{-1} for para-substituted benzene with no identical para (p)-pairs groups [169,170].
1465	Skeletal vibration of benzene ring.	Typical for p-substituted benzene with amine groups (NH_2) in both p-pairs [171].
1299	Carbon-nitrogen bond (C-N) stretching vibration.	Typical in the interval 1360-1250 cm^{-1} in secondary aromatic amines [169,172].
1184	Sulphone group ($-SO_3$) asymmetric stretching vibration.	Strong intensity band occurring typically at 1250-1140 cm^{-1} in sulphonic acid salts [169].
1130	Two possibilities: 1. Sulphate ion (SO_4^{2-}) stretching vibration. 2. Substituted benzene sulphonic acid salt.	Occurring typically at 1130-1080 cm^{-1}. Ionic sulphates, which are a common impurity, have a strong intensity band in this region [169].
1040	$-SO_3$ symmetric stretching vibration.	Sharp and strong intensity band occurring at 1070-1030 cm^{-1} in sulphonic acid salts [169].

Table 4.4 (continued).

Absorption wave number (cm^{-1})	**Assignment**	**Comments**
1011	Aromatic =C-H in-plane deformation vibration in p-substituted benzene.	Weak to medium intensity band [169,170].
830	Aromatic =C-H out-of-plane deformation vibration in p-substituted benzene.	Normally at 860-800 cm^{-1} [169,170].
689	Aromatic =C-H out-of-plane deformation vibration in p-substituted benzene.	Normally at around 695 cm^{-1} [169,170].
580	Scissoring vibration of the sulphonyl group ($-SO_2-$).	All sulphones have a characteristic band at 610-545 cm^{-1} [169,170].
502	Aromatic out-of-plane ring deformation vibration in p-substituted benzene.	Characteristic band at 520-445 cm^{-1} [169,170].

The results presented in Table 4.4 confirm the presence in the analysed sample of the polyaniline repeat unit, as depicted by the absorption peaks at 1465 and 1299 cm^{-1}. The OH peak at 3564 cm^{-1} exists because of residual water absorbed from the environment. The absorption peaks at 2956, 2924 and 2853 cm^{-1} are characteristic of functional groups corresponding to the alkane series, thus indicating the presence of this type of hydrocarbon chain in the sample. The use of a sulphonic acid or its derived salt as the doping agent is confirmed by the absorption peaks at 1184, 1130, 1040 and 580 cm^{-1}. Moreover, the absorption at 1130 cm^{-1} together with the ones at 1011, 830, 689 and 502 cm^{-1} strongly suggest that the doping agent may be in fact a para (p)-substituted benzene sulphonic acid or its derived salt. Furthermore, the presence of saturated aliphatic hydrocarbons chains in the sample suggests that these may be the substituent group in the benzene ring p-positions. The assumption that the absorption at 1612 cm^{-1} corresponds to the C=C stretching vibration in the aromatic ring of p-substituted benzene with no identical p-pair groups, reinforce even more the previous idea. On the other hand, if this peak were assigned to the N-H deformation vibration in primary

aromatic amines, then this would suggest that some non-polymerised aniline monomers might be present in the sample.

Despite the fact that the FTIR technique cannot yield a conclusive estimate about the size and isomeric structure of the hydrocarbons chain, all these results in conjunction with the results obtained from sections 4.3.1 and 4.3.2, reinforce the concept about the use of DBSA as the doping agent to yield electrically conductive polyaniline. The FTIR results presented are in good agreement with those presented by Levon et al. [72] and Hsu et al. [53] for polyaniline doped with DBSA.

The FTIR spectrum of the solution 1 (refer to section 4.3.1) is presented in figure 4.7.

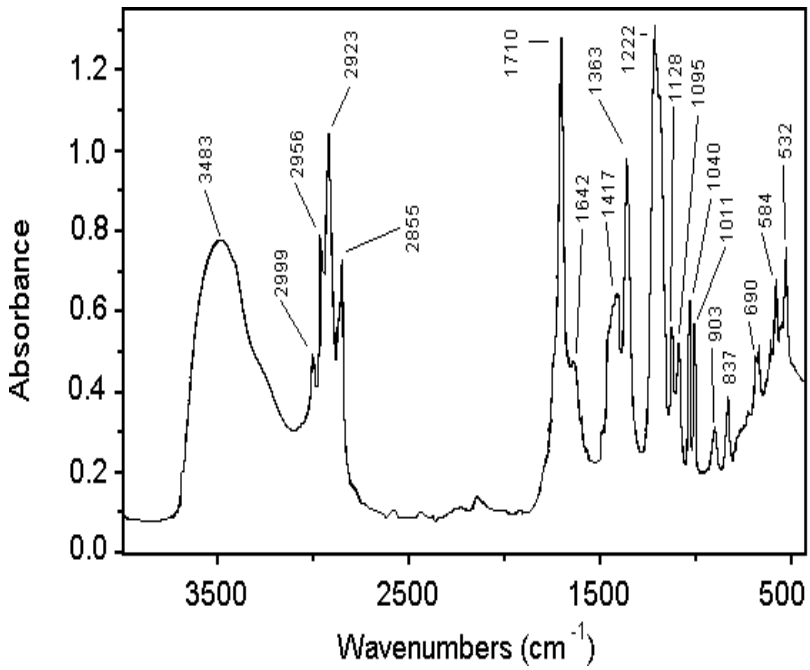

Figure 4.7. The FTIR spectrum of solution 1.

To facilitate the interpretation of the spectrum shown in fig. 4.7, a sample of clean acetone was also analysed by FTIR spectroscopy. The experimental conditions were the same as for the PANIPOL^{TM} pellets and solutions. The resultant spectrum (fig. 4.8) is as expected, with the characteristic absorption peaks for acetone [171]. The two FTIR spectra are overlapped in figure 4.9 to indicate better the identity of the chemical species extracted from the PANIPOL^{TM} pellets by the solvent. Figure 4.9 clearly indicates the identity of the functional groups present in solution 1. Accordingly, the

absorption peaks at 2999, 1710, 1417, 1363, 1222, 1095, 903 and 532 cm^{-1} are the characteristic ones for acetone (the peak at 784 cm^{-1} is overlapped by other absorption peaks of higher intensity).

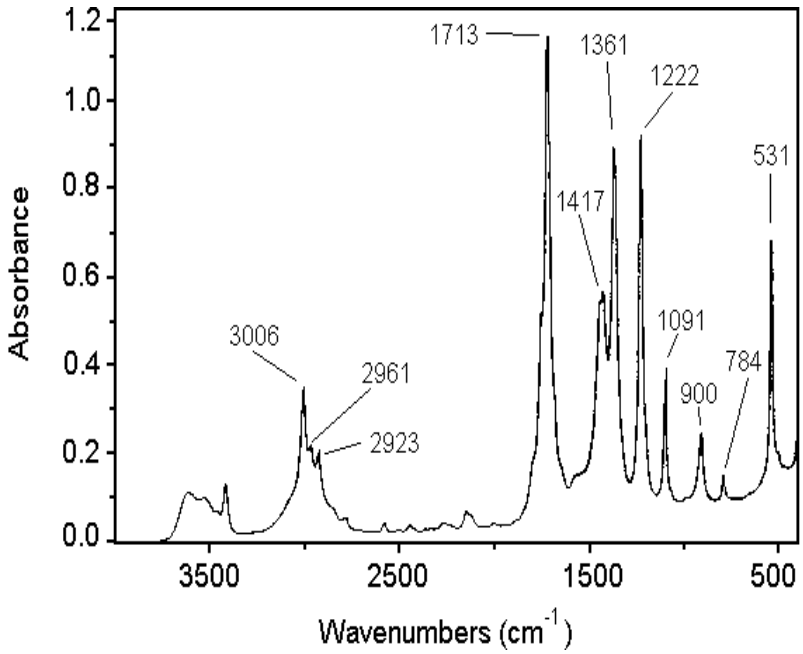

Figure 4.8. The FTIR spectrum of acetone.

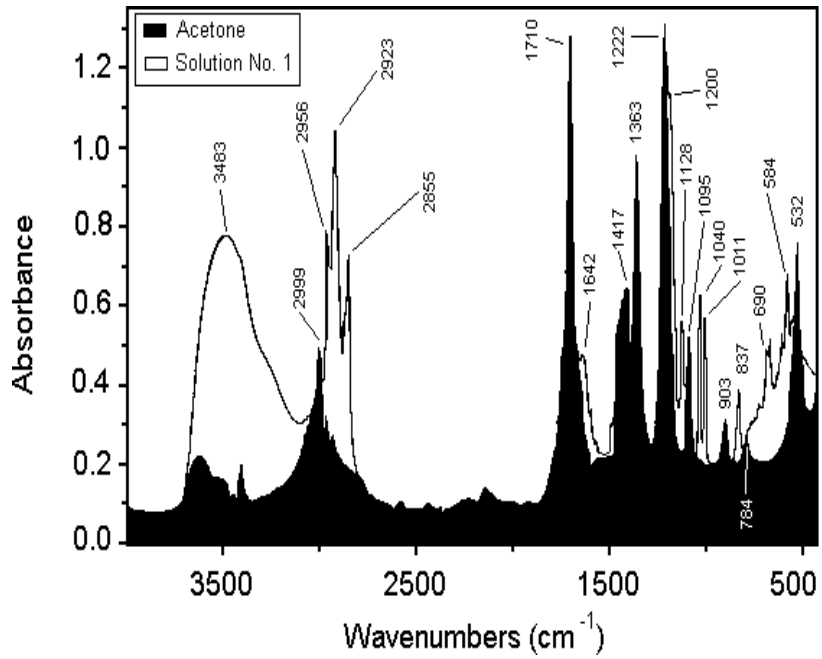

Figure 4.9. Comparison of the FTIR spectra of solution 1 and acetone.

The characteristic absorption peaks corresponding to the DBSA and its derived salt, also found in the spectrum of PANIPOL^{TM}, are also present in fig. 4.9, thus indicating the extraction of these compounds from the original PANIPOL^{TM} sample. The assignment of these peaks is as follows (refer to Table 4.4): 1128, 1040 and 584 cm^{-1} correspond to benzene-sulphonic acid salt, $-SO_3$ and $-SO_2-$, respectively. The absorption peak at 1200 cm^{-1}, partially overlapped by the absorption at 1222 cm^{-1}, is assigned to the $-SO_3$ asymmetric stretching vibration in sulphonic acid salts. The peaks at 2956, 2923 and 2855 cm^{-1} indicate the presence of $-CH_3$ and $-CH_2-$ in alkanes chains. The absorption peaks at 1011, 837 and 690 cm^{-1} are assigned to aromatic =C-H deformation vibrations in p-substituted benzene. Again, the peak at 3483 cm^{-1}, assigned to OH, appears as a result of residual water initially absorbed by the sample from the environment. The absorption at 1642 cm^{-1} could be due to C=N stretching vibration. This is characteristic of imines that generally absorb at a variable intensity at 1690-1640 cm^{-1}. However when there is an aromatic group attached to the nitrogen atom, the absorption appears near 1640 cm^{-1} [169]. This would indicate the extraction of quinoid groups possible present in the original PANIPOL^{TM} sample forming part of small amounts of undoped polyaniline.

The relative intensity of the majority of the absorption peaks corresponding to the above indicated functional groups decreased as the number of dissolution cycles in acetone was increased, indicating that the emeraldine salt in the original PANIPOL^{TM} sample was gradually being freed of the initially present DBS salt. For simplicity, only the FTIR spectra corresponding to solutions 3 (fig. 4.10) and 7 (fig. 4.11) are presented to exemplify this process. Figure 4.10 also shows the characteristic peaks for the salt of DBS, indicating that the sample was not totally free of this. However as can be observed, the absorption peaks corresponding to the acetone are more predominant. On the other hand, in fig. 4.11 it can be seen that the majority of the peaks present in the spectrum correspond to the acetone, indicating a lower content of DBS salt in the sample. The presence of the peaks at 1034 and 1009 cm^{-1} (for $-SO_3$ and aromatic =C-H, respectively), and some other ones overlapped in the 750-650 cm^{-1} interval (mainly for aromatic =C-H) suggests an incomplete extraction process. The presence of the peaks at 1650 cm^{-1} (C=N) in both spectra suggest the extraction of quinoid groups, originally

forming part of small amounts of undoped polyaniline. The peaks at around 3500 cm^{-1} (OH) appear as a result of residual water absorbed from the environment.

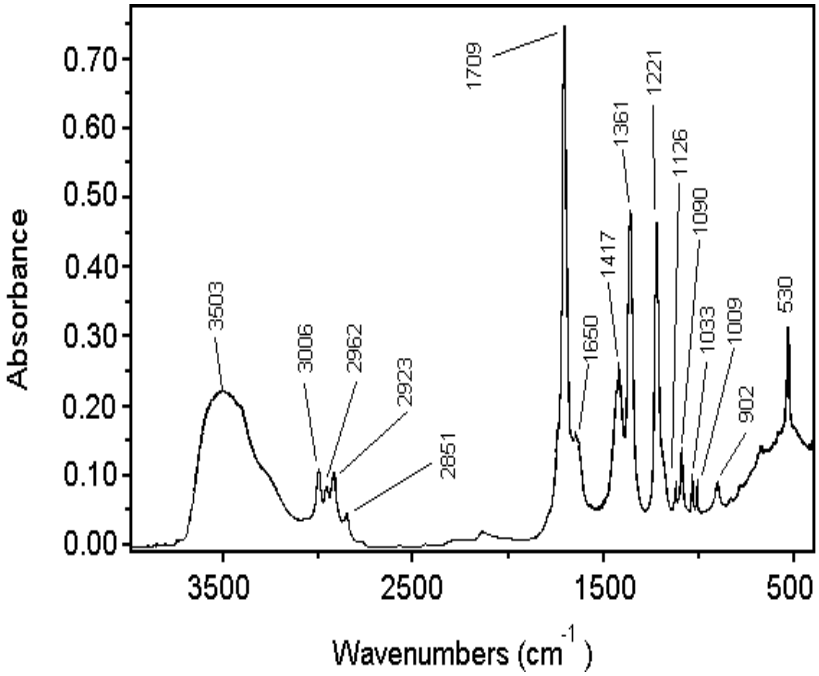

Figure 4.10. The FTIR spectrum of solution 3.

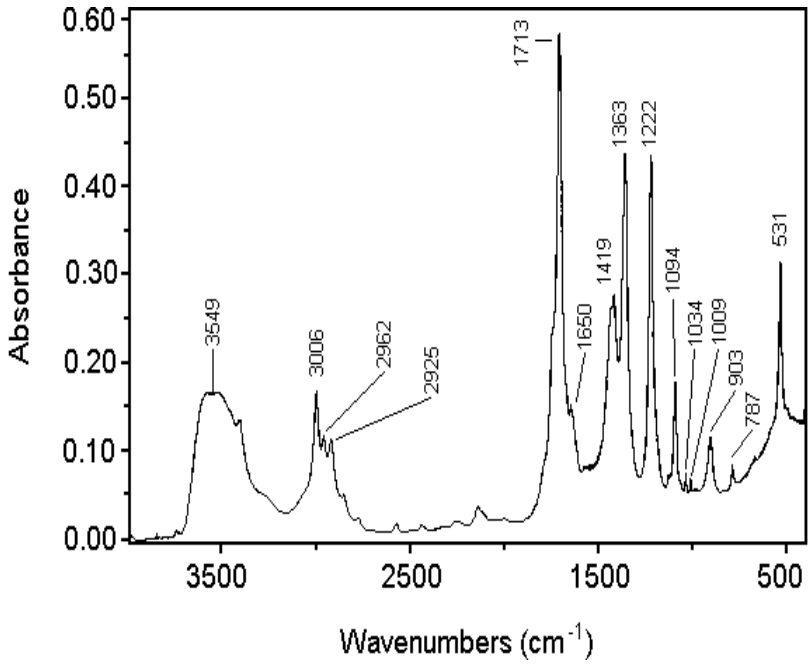

Figure 4.11. The FTIR spectrum of solution 7.

4.5 THERMAL ANALYSIS.

This analysis was carried out to have a better understanding about the thermal limitations of the PANIPOL^{TM} samples and, eventually, to assist in choosing the more suitable conditions for further processing. However, it should be pointed out, that thermal analyses like the ones described in the following sections cannot yield an absolute estimation of the nature and amounts of the components originally present in the samples. Therefore, the interpretation of the results is based on the scarce information provided by the manufacturer (concerning the composition of the samples and type of some components), the experimental results detailed in the previous sections and the findings reported in the literature concerning conductive polyaniline systems presumably similar to the present ones.

4.5.1 THERMOGRAVIMETRIC ANALYSIS.

The thermal stability of the three PANIPOL^{TM} samples within the temperature range from 40 to 750°C was investigated using a Perkin-Elmer TGS-2 thermogravimetric analyser (TGA). For each PANIPOL^{TM} sample, two samples of about 4.0 mg of the powdered pellets were analysed at a rate of 10°C/min under a nitrogen atmosphere. The pellets were pulverised with a pestle and mortar.

Selected TGA thermograms of the samples 1 and 2 of PANIPOL^{TM} are presented in figures 4.12 and 4.13, respectively. On the other hand, a selected thermogram of PANIPOL^{TM} 3 is depicted in figure 4.14. Figures 4.12 and 4.13 show that the thermograms of the samples 1 and 2 of PANIPOL^{TM} are very similar. The thermograms show that the sample weight is gradually lost up to a temperature of about 250°C. As the samples were not previously dried, this small weight loss (about 2.8 %) is presumably due to the loss of water absorbed from the environment. It is also possible that the loss of low molecular weight oligomers initially present in the sample contribute to this wt. % loss.

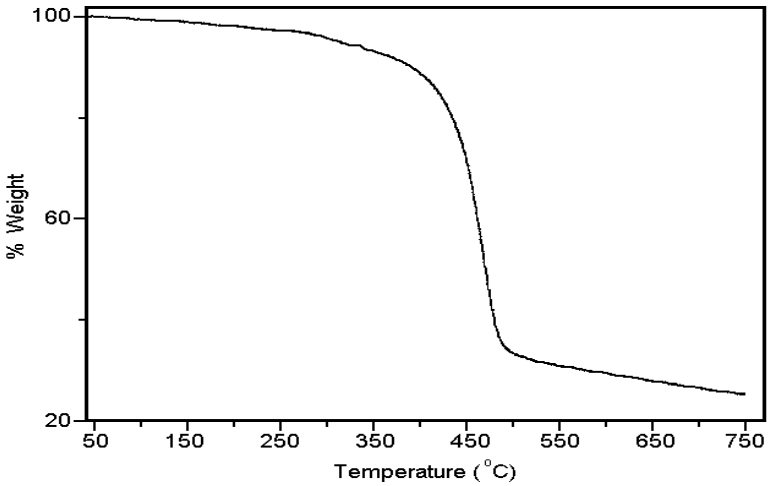

Figure 4.12. The TGA thermogram of PANIPOL™ 1.

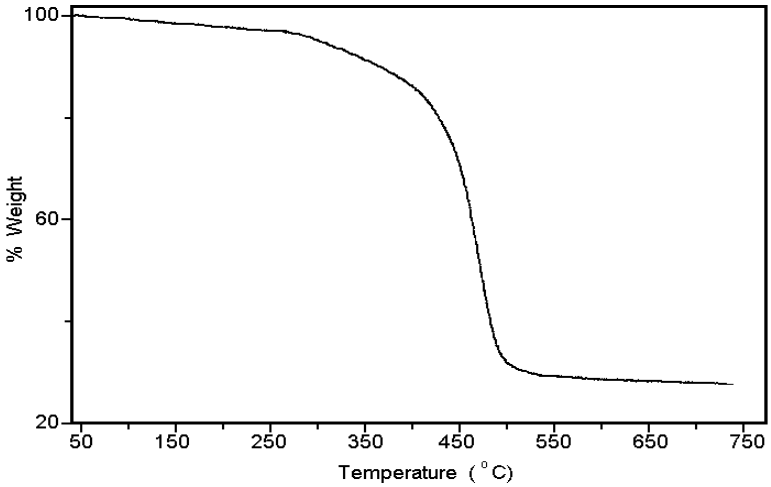

Figure 4.13. The TGA thermogram of PANIPOL™ 2.

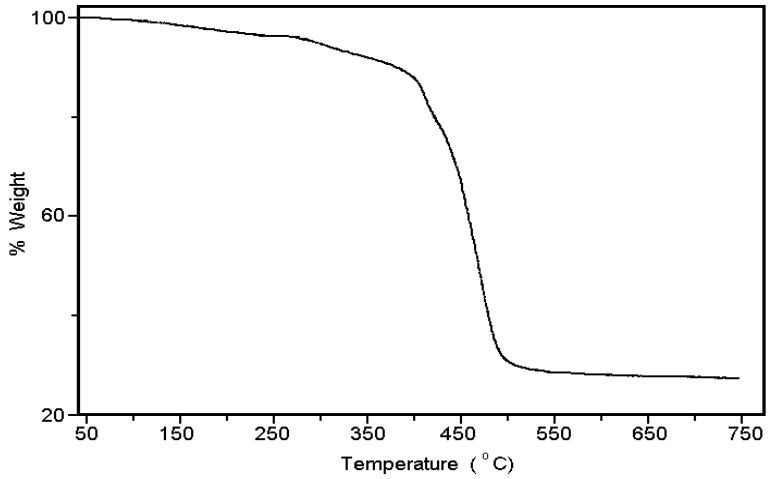

Figure 4.14. The TGA thermogram of PANIPOL™ 3.

The thermogram of PANIPOL^{TM} 2 also suggests that between about 250 and 540°C an abrupt weight loss is observed (ca. 69 %). This temperature range shows two step-like sections, one occurring between about 250 and 390°C, and another one taking place between about 390 and 540°C. The first of these sections represents about 15 % of the total weight loss that occurs in this range of temperature. It is believed that this wt. % corresponds to the dopant loss. This is based on the fact that about 0.5 mol of protonic acid per mol of phenyl-N repeat unit of polyaniline is needed [65] for obtaining a fully protonated conductive complex. Assuming that the protonic acid used is DBSA, then a fully protonated complex would be composed of ca. 64 wt. % of DBSA and 36 wt. % of polyaniline repeat unit. Taking into account that the polyaniline salt (the protonated complex) is only about the 25 wt. % of the analysed sample (the rest is the Zn compound), then the DBSA used as the dopant agent, and bound to the polyaniline backbone, would represent only about 16 wt. % of the whole sample. This weight percent is not very different to the 14.5 wt. % loss observed in the range 250-390°C, thus reinforcing the above mentioned observation. The second section, corresponding to about 85.5 % of the total wt. loss observed in the range 250-540°C, represents the degradation of the polymer and the Zn salt of DBS. This agrees very well with the thermal properties of doped polyaniline reported by some manufacturers (for example, Ormecon Chemie GmbH & Co. [173] reports on a degradation process starting at 320°C). Above 540°C only about the 28 % of the original weight of the sample is left, corresponding to decomposition products, mainly containing Zn and carbon atoms.

As observed in fig. 4.12, the TGA thermogram of PANIPOL^{TM} 1 is similar to that of PANIPOL^{TM} 2. Small differences can be noticed however. This is especially observed in the range of temperatures at which an abrupt weight loss is observed, that is, for PANIPOL^{TM} 1, this takes place between about 250 and 510°C (about 64 wt. % loss), whereas for PANIPOL^{TM} 2 this occurs in the range 250-540°C. However, as with PANIPOL^{TM} 2, the 250-510°C range depicted in the thermogram of PANIPOL^{TM} 1 is also divided into two sections occurring at similar temperatures to those for PANIPOL^{TM} 2. In general, the weight percentages representing those sections are very similar to those for PANIPOL^{TM} 2. The events taking place in PANIPOL^{TM} 1 are believed to be of the same nature as those occurring in PANIPOL^{TM} 2. The differences found may originate from slight differences in the samples' composition.

With respect to PANIPOL^{TM} 3, its TGA thermogram (fig. 4.14) also differs, to some extent, from those of the samples 1 and 2. For instance, the characteristic initial gradual weight loss occurs up to about 240°C, and what is more, that loss of weight represents about 3.8 %, differing with the observed for the other two samples (about 2.8 %). Moreover, at about 240°C, the thermogram shows a step-like stage in which the sample weight is constant with respect to the temperature. This is maintained for over a range of about 25°C after which the sample weight is abruptly lost. After this, the thermogram shows again a similar fashion to that shown in those of the samples 1 and 2. Once more, the events taking place in PANIPOL^{TM} 3 are believed to be of the same nature as those occurring in the previous samples. The differences found may have resulted from differences in the samples' composition.

Overall, the TGA thermograms presented in figs. 4.12 to 4.14 compare very well with the one reported by Zilberman et al. [21] for polyaniline doped with DBSA.

In general, these results, as also indicated by the manufacturer [71], suggest that the PANIPOL^{TM} samples could be safely processed up to a maximum temperature of about 250°C without exposing them to severe degradation and loss of their electrically conductive characteristics.

4.5.2 DIFFERENTIAL SCANNING CALORIMETRY.

The thermal behaviour of the three PANIPOL^{TM} samples over the range of temperature from 325 to 680 K (52 to 407°C) was initially investigated using a Perkin-Elmer DSC-2C Differential Scanning Calorimeter (DSC). For each PANIPOL^{TM} sample, two samples of about 5 mg of the powdered pellets were analysed at a rate of 10°K/min under a nitrogen atmosphere. During the experiments, one of the calorimeter pans was kept empty as a reference. Before performing the experiments, a base line was run keeping empty the two calorimeters' pans. The base line was subtracted from the resultant data corresponding to the samples and heat flow-temperature plots were produced. The experiments, data collection and numerical calculations were performed

using the software 2-Series/TADS DSC-2C. The pellets were pulverised with a pestle and mortar.

The thermal behaviour of the three PANIPOL^{TM} samples during exposure to a heating-cooling-heating cycle was also analysed. For this, the analysis of the pulverised pellets was performed in a Perkin-Elmer DSC-7 Differential Scanning Calorimeter. The data collection and numerical calculations were carried out using the software 7-Series/UMX DSC-7. For each PANIPOL^{TM} sample, two samples of about 5 mg were heated at rate of 10°C/min from 35 to 220°C. Immediately after reaching the maximum temperature, the samples were cooled down to the initial temperature at a rate of 5°C/min. Afterwards they were heated up again to the maximum temperature at rate of 10°C /min. The experiments were performed under a nitrogen atmosphere. Similar experiments to the ones just above described were carried out on the three PANIPOL^{TM} samples in the range of temperatures from 35 to 110°C. Two samples of each conductive complex were heated at rate of 10°C/min. The samples were kept for 10 min at the maximum temperature, after which they were cooled down to 35°C at a rate of 5°C/min. The samples were kept at this temperature for 0.5 min and afterwards they were heated up again to the maximum temperature at rate of 10°C /min. The experiments were also performed under a nitrogen atmosphere.

The resultant sediment from the last dissolution cycle of PANIPOL^{TM} 2 in acetone (refer to section 4.3.1) was also thermally analysed over the range of temperatures from 35 to 220°C. The analysis was performed using the instrument and software mentioned in the previous paragraph. Two samples of about 5 mg were heated at a rate of 10°C /min under a nitrogen atmosphere.

All the PANIPOL^{TM} samples analysed over the range of temperatures from 325 to 680°K (52 to 407°C) presented a very similar thermal behaviour. For simplicity, only a selected DSC thermogram (PANIPOL^{TM} 2) is presented in figure 4.15. This figure shows a broad endotherm between about 75 and 110°C. As the samples were not previously dried this endotherm is mainly attributed to the evaporation of water absorbed from the environment. An exothermic range is observed between about 140 and 150°C. Kärnä et al. [164] and Levon et al. [72] observe that this is characteristic for polyaniline doped with DBSA at a PANI:DBSA weight ratio of about 1:2.5. Moreover,

they mention that the reason for this is a homogeneous phase transition occurring in the doped complex in a range of temperatures from 110 to 170°C.

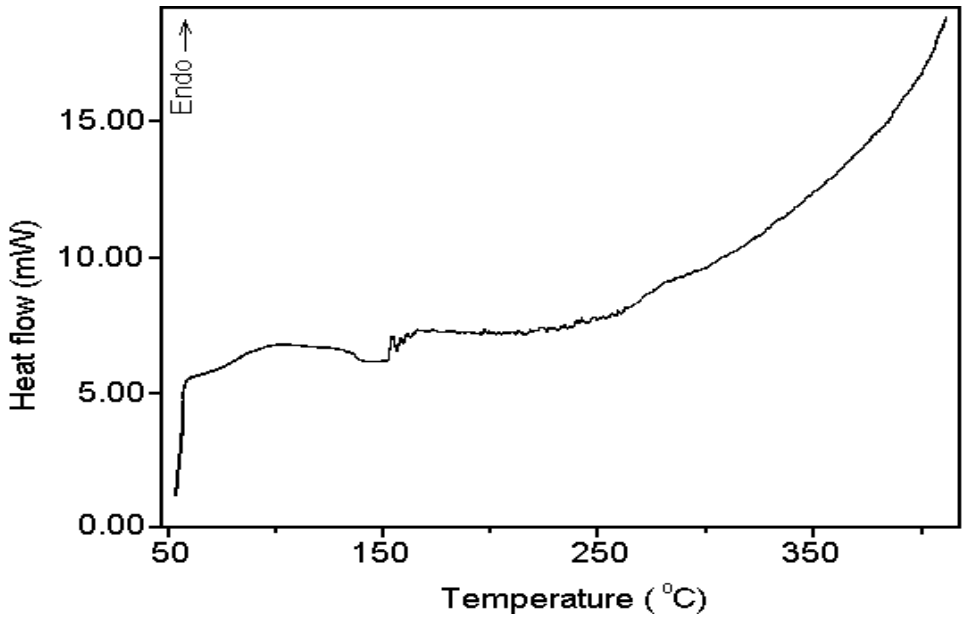

Figure 4.15. The DSC thermogram of the powdered PANIPOL™ pellets.

In fig. 4.15, a group of endotherms is observed between about 150 and 250°C. The cause of these could be attributed to transitions in the internal structure of additives present in the sample. As in the TGA analysis, it is possible that loss of low molecular weight oligomers also occurs in the range 75-250°C. Above about 250°C, a constant rising endotherm is observed which is attributed to the loss of the doping agent, and polymer and Zn compound degradation. Further complexation of DBSA with polyaniline may also occur in addition to possible crosslinking and other reactions. As has been seen, these results are in well agreement with those obtained from the TGA experiments regarding a “safe” processing temperature range. None of the above observed endotherms are associated with the melting of polyaniline as this polymer does not exhibit this type of thermal phase transition but instead only soften and then decomposes at about 320°C (see for example reference 173). Similarly, providing that all the polyaniline molecules present in the sample are doped, then none of the endothermic regions would correspond to the glass transition of polyaniline as the complexation of this with the DBSA decreases the temperature at which this occurs to

about –20°C [164]. The DSC thermogram of PANIPOL^{TM} presented in fig. 4.15 compares well with the observations reported by Zilberman et al. [21] on the thermal behaviour of polyaniline doped with DBSA.

The resultant thermal behaviour of all the PANIPOL^{TM} samples exposed to the heating-cooling-heating cycle in the range of temperatures from 35 to 220°C was very similar. For simplicity, only a selected DSC thermogram (PANIPOL^{TM} 2) is presented in fig. 4.16. This figure shows in more detail the endothermic and exothermic regions in the aforementioned safe processing temperature range (1st. heating scan). Again, the endotherms between about 75 and 110°C are attributed to moisture and possible loss of low molecular weight oligomers. The exothermic range characteristic of the polyaniline-DBSA complex is again present at about 130-140°C, and the endotherms associated with transitions in the internal structure of additives, other possible reactions and yet further loss of oligomers are present at above about 140°C. However, it is interesting to note that the heat absorption during the occurrence of the latter endotherms tend to decrease as the temperature is increased, slightly differing from the observed in the thermogram of the same sample (PANIPOL^{TM} 2) analysed over a wider range of temperatures (fig. 4.15). This discrepancy may be associated to an inhomogeneous distribution of the components (especially those of additive nature) in the sample during the manufacturing process. The same observations apply to the other samples (PANIPOL^{TM} 1 and 3).

Figure 4.16 also shows that the endothermic and exothermic regions observed during the first heating scan do not appear during the cooling scan at 5°C/min. This confirm the previous observations concerning the nature of the events taking place during the heating of the samples, namely that these are not thermal phase transitions (e.g., glass transition and/or melting in the case of endotherms), but mainly evaporation of water and loss of additives. The absence of endothermic and exothermic regions during the second heating scan after cooling reinforces the above mentioned observation. Moreover, this suggests that modifications in the microstructure of the doped complex have taken place. This, in principle, would suggest that the samples do not maintain their intrinsic properties even when exposed to the so-called safe processing range of temperatures, implying that there is a limitation regarding the number of heating cycles and hence, limitations on their reprocessability.

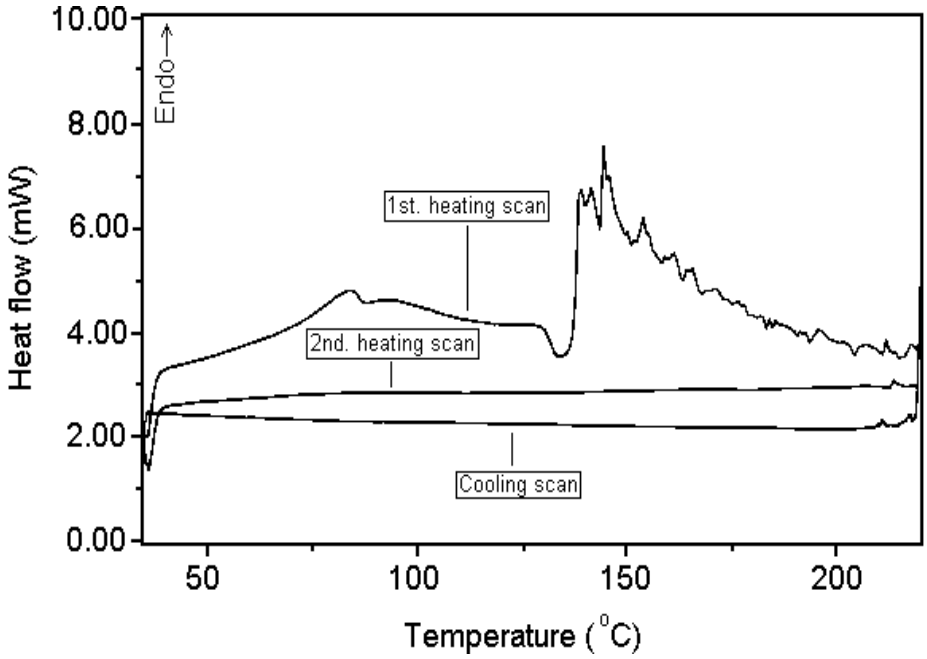

Figure 4.16. The heating-cooling-heating DSC thermogram of PANIPOL™ in the range of temperatures from 35 to 220°C.

The resultant thermal behaviour of the three PANIPOL™ samples exposed to the heating-cooling-heating cycle in the range of temperatures from 35 to 110°C is presented in fig. 4.17. From this figure, it can be observed that, in contrast with the observed in the range of temperatures from 35 to 220°C, the samples thermal behaviour showed some differences. For example, the first heating scan in the thermogram of PANIPOL™ 1 shows what it seems to be a melting peak at about 88°C. This is confirmed by the crystallisation peak at about 70°C in the cooling scan and further reappearance of the melting peak at about the same temperature (88°C) in the second heating scan. In contrast, the thermograms of PANIPOL™ 2 and 3 do not indicate these thermal transitions in the samples during the same analysed range of temperatures. Moreover, the thermograms of PANIPOL™ 2 and 3 show some similarities. That is, two almost imperceptible endothermic regions at about 80 and 100°C. These endotherms, as also observed in fig. 4.16, may be associated with moisture and possible loss of low molecular weight oligomers.

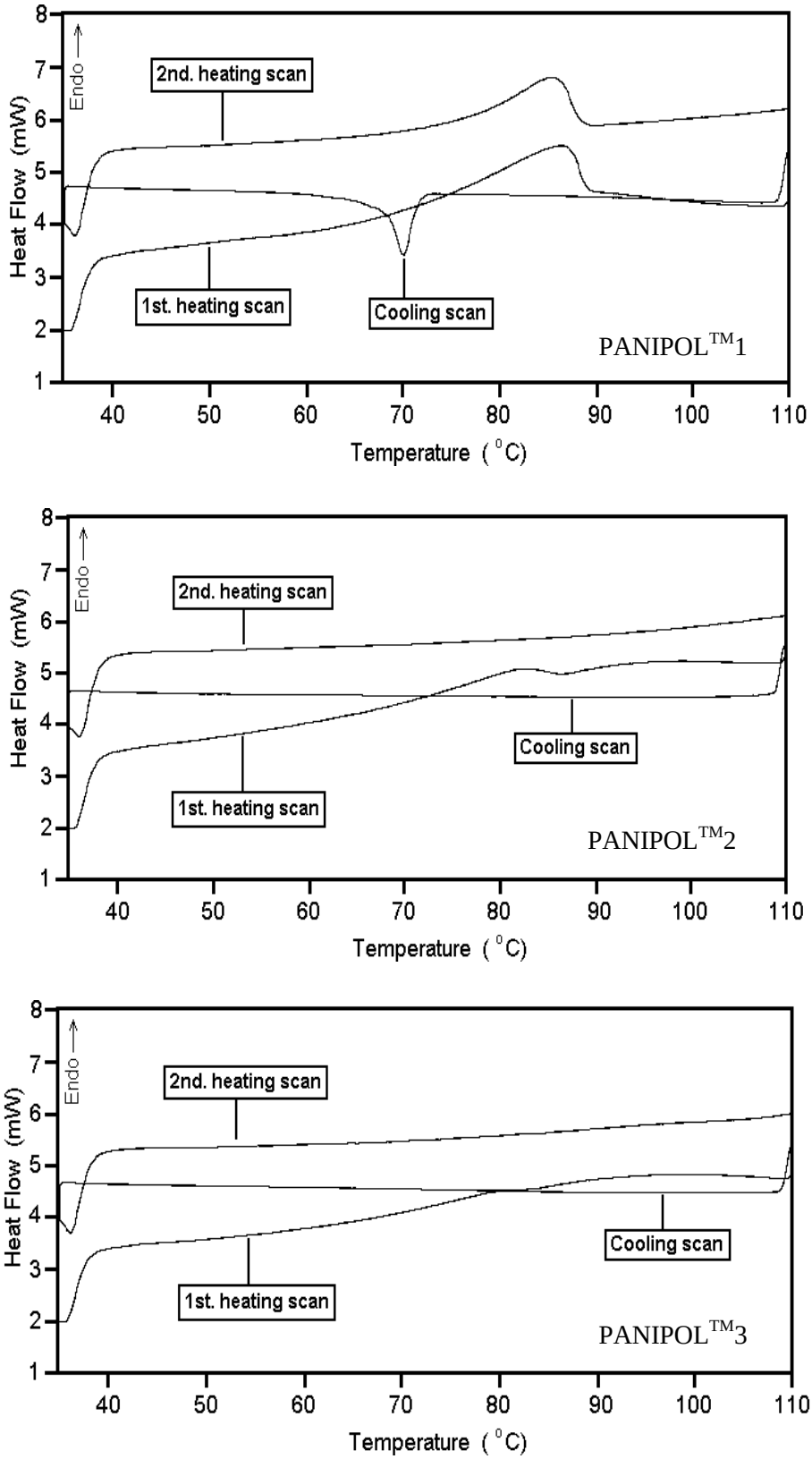

Figure 4.17. The heating-cooling-heating DSC thermograms of the PANIPOL™ samples in the range of temperatures from 35 to 110°C.

It is believed that the endotherms observed in the thermogram of PANIPOL™ 1 (fig. 4.17) represent the melting point of a certain additive present in the sample and that was not used in the preparation of the samples 2 and 3. In addition, this compound may decompose at a temperature between 110 and 220°C. This is because exothermic and endothermic regions were not found, respectively, in the cooling and second heating scans carried out in the range 35-220°C (fig. 4.16). These findings reinforce even more the concept about limitations on the samples reprocessability in this range of temperatures.

A selected DSC thermogram corresponding to the resultant sediment from the last dissolution cycle of PANIPOL™ 2 in acetone (refer to section 4.3.1) over the range of temperatures from 35 to 220°C is presented in figure 4.18. A thermogram of the original undissolved sample is also presented for comparison.

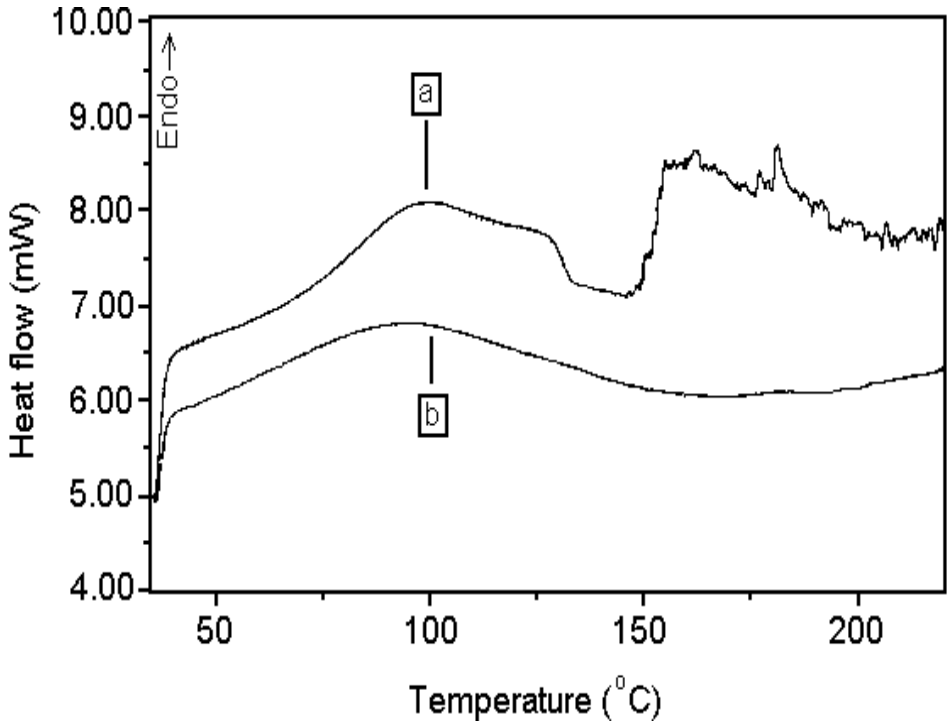

Figure 4.18. Comparison between the DSC thermograms of PANIPOL™ 2 (a) and the final sediment obtained from its dissolution in acetone (b).

In fig. 4.18, the thermogram corresponding to the undissolved sample of PANIPOL™ 2 shows the endothermic and exothermic regions above discussed. However, comparing this thermogram with that shown in fig. 4.16 corresponding to a

similar sample of the undissolved PANIPOL™ 2 pellets, some disagreement is found regarding the heat absorption level and its trend in the endotherms occurring beyond about 140°C. This suggests again, an inhomogeneous distribution of components in the sample during the manufacturing process. The thermogram corresponding to the sediment shows an endothermic region between about 75 and 125°C mainly corresponding to evaporation of moisture. The presence of the characteristic exothermic region at 130-140°C for the doped polyaniline complex is not very clear. However, the separation of this, during its dissolution in acetone, from the rest of the components originally present in the PANIPOL™ 2 pellets is exemplified by the absence of their attributed endotherms occurring beyond 140°C.

4.6 RHEOMETRY.

These experiments were performed to understand the flow properties of the materials in their molten state under different levels of shear rate. The results from the analysis would, eventually, be the main support when establishing the materials' processing parameters. Consequently, the rheological behaviour of the three PANIPOL™ samples, LDPE, PP and SBS was investigated using a Davenport extrusion rheometer with a piston diameter of 19.05 mm. The Poiseuille Law for capillary flow [174,175] was used to calculate the apparent shear viscosity (η) at different apparent wall shear rates $(\dot{\gamma})$ and temperatures for each material. Accordingly, η and $\dot{\gamma}$ were calculated using the following equation:

$$\eta = \frac{\tau}{\dot{\gamma}} = \frac{Pr/2L}{4Q/\pi r^3} = \frac{\pi P r^4}{8LQ} = \frac{\pi P r^4}{8LVA} \quad \text{.....Eq. 4.4,}$$

where:

τ = wall shear stress[1],

P = Pressure at the entrance of the capillary,

r = capillary radius,

L = capillary length,

[1] Note: No end pressure drop correction [174,175] was performed for the calculation of this parameter.

Q = volume flow rate,
V = piston drive speed, and
A = area of the piston ram.

For the experiments, the materials were extruded using a capillary die with an L = 35 mm and an r = 0.8 mm. The analysis was performed at selected piston drive speeds ranging from 0.25 to 50.00 mm/min. At each extrusion speed, the pressure sensed by a transducer, situated near to the entrance of the capillary die (refer to figure 4.19), was recorded for the calculations. To ensure that the materials were fluid enough to pass through the capillary, these were extruded, at the prefixed temperature, after 10 min of being into the rheometer barrel. To perform the experiments, an adequate amount of material to fill the barrel up to about its maximum capacity was used.

The rheological behaviour of the PANIPOL™ samples was analysed at 80, 100, 120 and 150°C, while for SBS the analysis was performed at 100, 120 and 150°C. LDPE and PP were analysed at temperatures above their melting point. Consequently LDPE was extruded at 120 and 150°C, while PP was analysed at 170, 180 and 190°C.

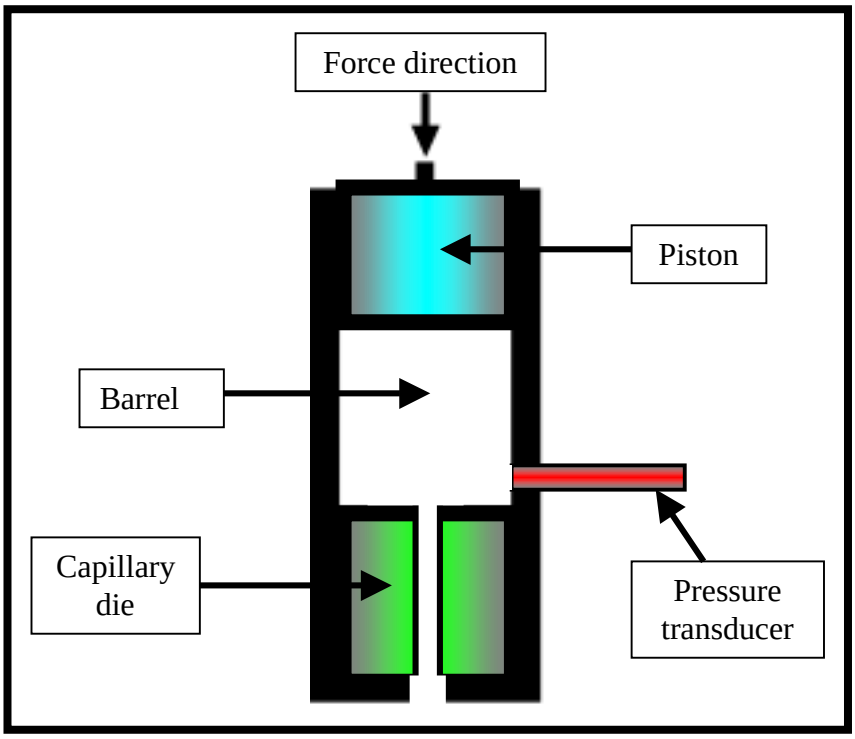

Figure 4.19. Diagram showing the main parts of the extrusion rheometer.

The extrusion of the samples 2 and 3 of PANIPOL^{TM} at 80°C was not possible even at the lowest piston drive speed *(V)* of 0.25 mm/min. It was initially anticipated that this could happen as the processing temperatures recommended by the supplier [71] range from 100 to 225°C. However, experiments were performed at 80°C because, as also suggested by the manufacturer, the recommended processing temperatures could vary depending on the equipment used. During the experiments, it was observed that the pressure increased until it reached a level close to the transducer safety limit of 27.58 x 10^{6} N/m^{2}. This also happened during the extrusion of SBS at 100°C, and PP at 170 and 180°C. The reason for this is that the materials were not fluid enough to pass through the capillary die. Also, it is possible that the geometry and dimensions of the die were not the appropriate ones for the extrusion of the materials at those speeds and temperature conditions.

Regarding PANIPOL^{TM} 1, its extrusion was accomplished at all the intended temperatures, even at the lowest one (80°C). This fact initially indicated that this sample was less viscous than PANIPOL^{TM} 2 and 3. As will be seen later, this was the case at all comparable extrusion conditions.

In general, it was observed that the extrudates of the three PANIPOL^{TM} samples were very brittle and their surface finish was poor. This was observed at all the extrusion conditions. However, the degree of brittleness was more evident at lower extrusion speeds and at higher temperature levels. For example, at 150°C and 0.25 and 2.5 mm/min it was not possible to obtain a continuous piece of a PANIPOL^{TM} 2 extrudate though at this same temperature, but at 5 mm/min some small continuous fragments were obtained. On the other hand, the quality of the finish especially decreased at higher extrusion speeds and temperature levels. Overall, it was observed that the quality of the extrudates of PANIPOL^{TM} 2 was relatively better than that of those corresponding to PANIPOL^{TM} 1 and 3 obtained at comparable extrusion conditions. In general, extrudates of better quality were produced at 120°C. However, as can be seen in figure 4.20, during the extrusion of PANIPOL^{TM} 2 at 5 mm/min, the pressure increased with time until it reached a stage at which erratic behaviour was displayed. This type of behaviour, also observed during all the extrusion conditions, reflects the already discussed poor quality of the extrudates. Also, it is believed that this relates to the composition of the extruded pellets, thus suggesting that they are not

homogenous. The aforementioned erratic behaviour of pressure was also observed during all the extrusion conditions of the other two PANIPOL™ samples, indicating that they are not homogeneous.

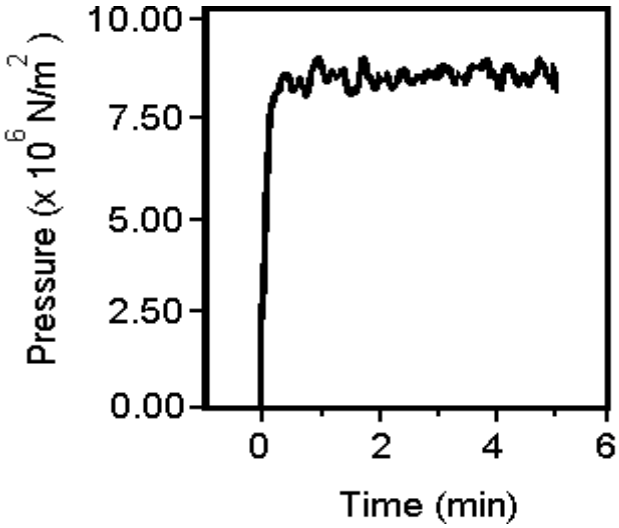

Figure 4.20. Variation of pressure with time during the extrusion of PANIPOL™ 2 at 5 mm/min and 120°C.

It is also possible that the irregular behaviour of pressure is due to reactions taking place among certain components that were possibly in excess in the pellets, thus suggesting that the material is relatively unstable. All this is supported by observing the behaviour of pressure displayed for materials known to be stable and whose compositions are homogeneous. For example, figure 4.21 shows that during the extrusion of SBS and LDPE the pressure increases until it reaches a constant level, differing from what is observed for PANIPOL™ 2 extruded under the same conditions. These results are in good agreement with the results and observations generated from the thermal analysis about an inhomogeneous distribution of components in the sample during the manufacturing process. Moreover, the poor quality of the extrudates, especially those obtained at higher levels of temperature, support the observations about the loss of important additives (perhaps compatibility agents). It should be mentioned, however, that despite the above discussed erratic behaviour of pressure, a constant trend of this with respect to time was observed in the majority of the cases (see for example figs. 4.20 and 4.21). An estimated average value of pressure in the “erratic interval” was

used in *Eq. 4.4* for the calculations. Additional examples of the typical erratic behaviour of pressure with time are presented in the appendix No. 1 in which the reader is provided with some selected experimental pressure vs. time charts for further consult.

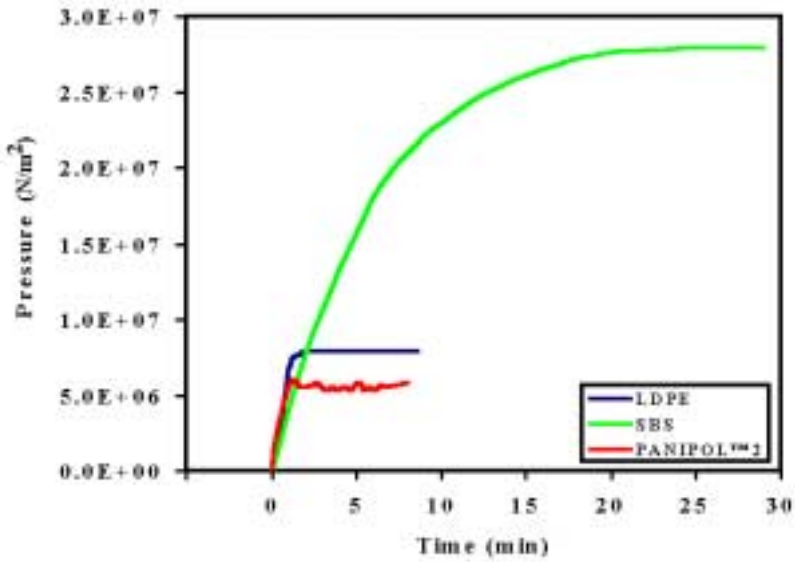

Figure 4.21. Variation of pressure with time during the extrusion of PANIPOL™ 2, SBS and LDPE at 1.25 mm/min and 120°C.

Wall shear stress values at each apparent wall shear rate level were calculated for the three PANIPOL™ samples, at each of their corresponding extrusion temperatures, using *Eq. 4.4*. Similarly, the apparent viscosity was calculated using the same equation and the values obtained for τ and $\dot{\gamma}$. For PANIPOL™ 1, the results corresponding to the extrusion temperature of 80°C are presented in figure 4.22 as a η-$\dot{\gamma}$ log-log plot. In a similar manner, the results corresponding to the extrusion temperatures of 100, 120 and 150°C are presented in figures 4.23 to 4.25, respectively. For comparison, the results corresponding to PANIPOL™ 2 and 3 are also included in these figures. The results suggest that the PANIPOL™ samples behave like a material obeying the power law (which is commonly proposed to describe pseudoplastic behaviour [174,175]) in the experimental $\dot{\gamma}$ interval from about 3.6 to 717 s^{-1} (that is, V = 0.25 to 50.00 mm/min). This is observed especially at the extrusion temperatures of 100 and 120°C. This is clearly exemplified in figs. 4.22 to 4.24, which shows that the experimental data are very well fitted by the power law equation. At 150°C (fig. 4.25), PANIPOL™ 1 and 3 still exhibit pseudoplastic behaviour. However at that same temperature, the

experimental data corresponding to PANIPOL™ 2 seems to deviate from the behaviour displayed at lower extrusion temperatures. In general, the results presented indicate that PANIPOL™ 2 and 3 exhibit similar levels of viscosity at all comparable extrusion conditions, being PANIPOL™ 2 the most viscous of the samples.

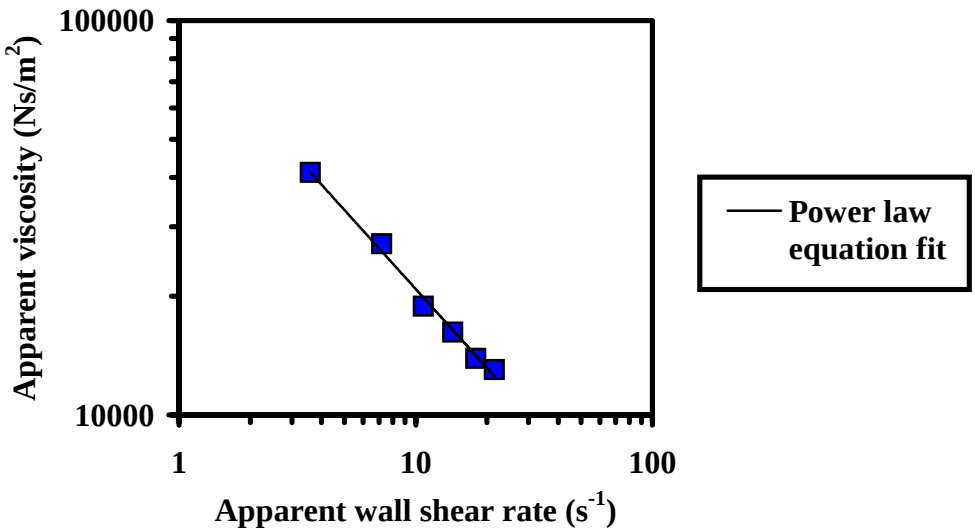

Figure 4.22. Variation of the apparent viscosity with respect to apparent wall shear rate for PANIPOL™ 1 capillary extruded at 80°C.

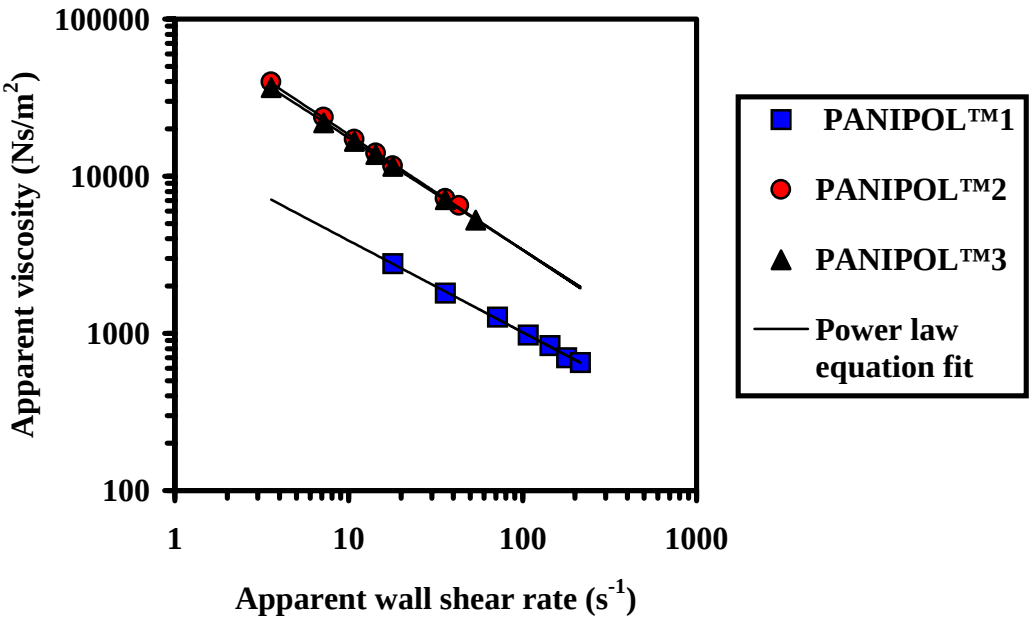

Figure 4.23. Variation of the apparent viscosity with respect to apparent wall shear rate for the PANIPOL™ samples capillary extruded at 100°C.

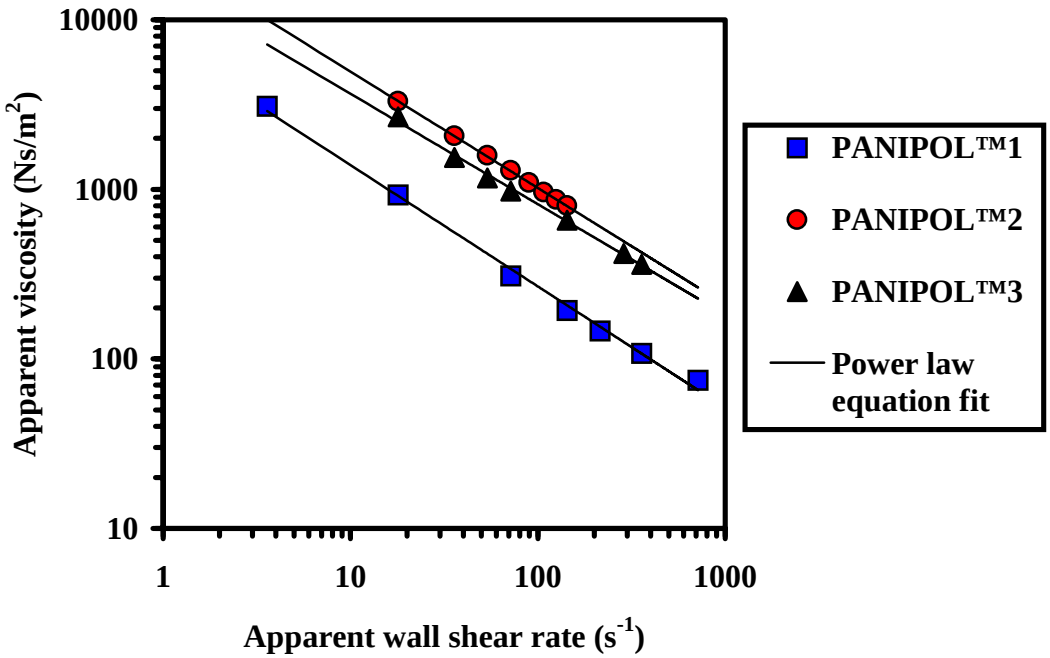

Figure 4.24. Variation of the apparent viscosity with respect to apparent wall shear rate for the PANIPOL™ samples capillary extruded at 120°C.

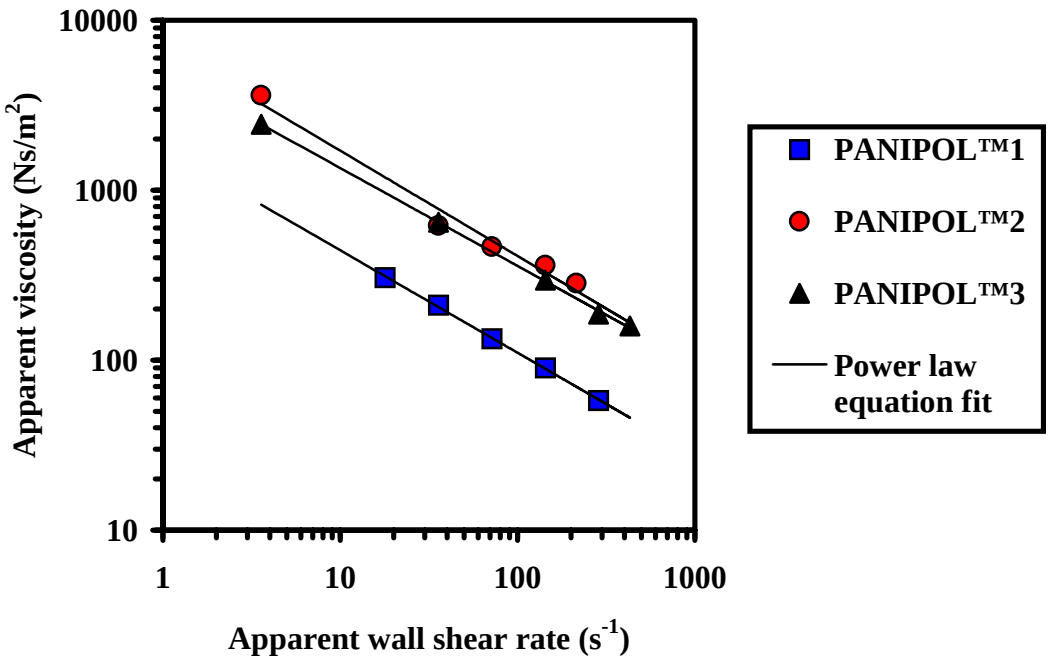

Figure 4.25. Variation of the apparent viscosity with respect to apparent wall shear rate for the PANIPOL™ samples capillary extruded at 150°C.

The apparent viscosity of SBS and LDPE at 120 and 150°C was calculated at different apparent wall shear rates using *Eq. 4.4* and the values of pressure recorded during the experiments at each extrusion speed. The results are presented in figs. 4.26 and 4.27 as log-log plots of η versus $\dot{\gamma}$.

For comparison purposes, figs. 4.26 and 4.27 also include the rheological behaviour of the PANIPOL™ samples analysed at the same extrusion temperatures. It can be seen that, similarly to what is observed for the PANIPOL™ samples, the viscosity of the two insulating polymers decreases with increase of temperature and shear rate. The form in which the viscosity decreases with respect to the shear rate indicates that the SBS and LDPE behave as pseudoplastic fluids obeying the power law in the specific $\dot{\gamma}$ intervals. The SBS is the most viscous of the materials at all comparable experimental conditions, whereas the PANIPOL™ samples proved to be the least viscous ones. However, the viscosities of the LDPE and PANIPOL™ 2, specifically at 120°C, are of a similar magnitude.

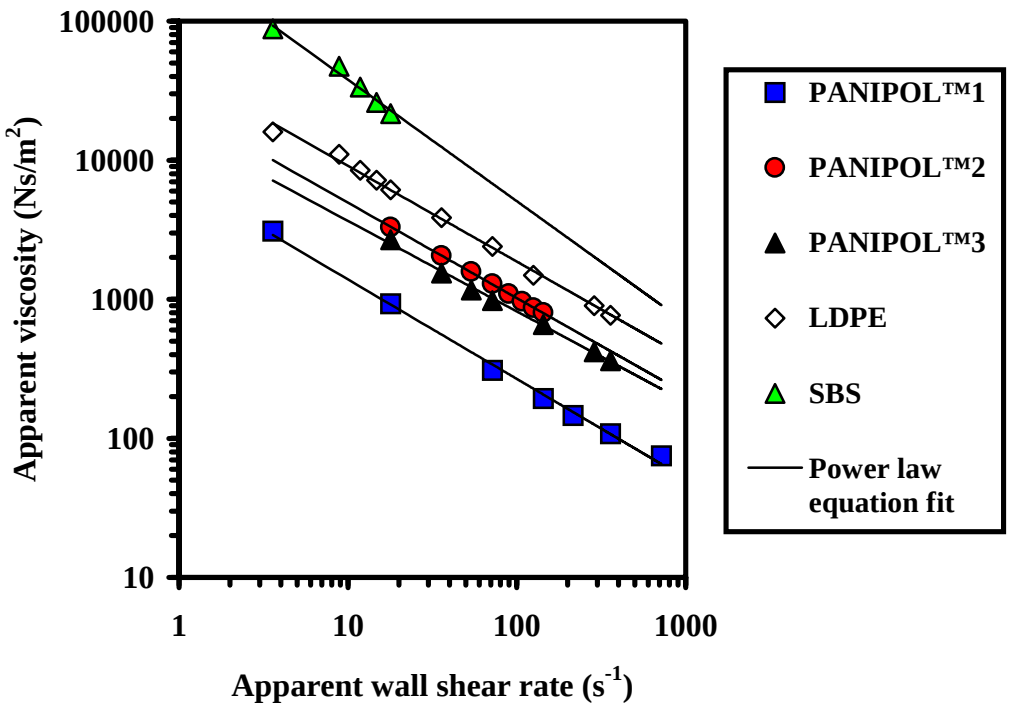

Figure 4.26. Variation of the apparent viscosity with respect to apparent wall shear rate for the LDPE, SBS and PANIPOL™ samples capillary extruded at 120°C.

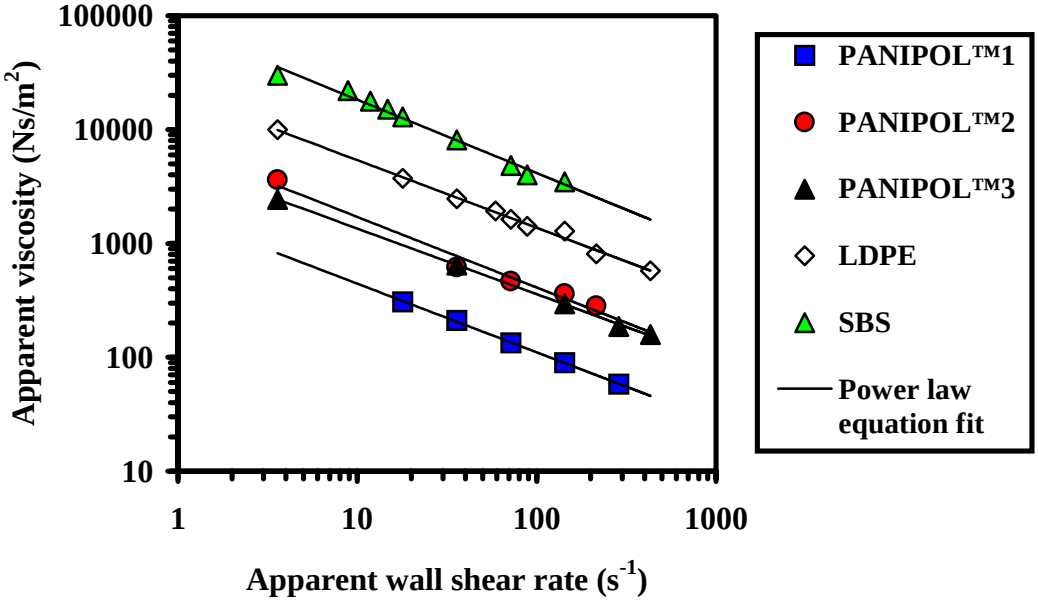

Figure 4.27. Variation of the apparent viscosity with respect to apparent wall shear rate for the LDPE, SBS and PANIPOL™ samples capillary extruded at 150°C.

The calculations of the apparent viscosity for the PP extruded at 190°C was performed in a manner similar to that described for the previous materials. The results are presented in fig. 4.28, which also shows the rheological behaviour of the PANIPOL™ samples at 150°C.

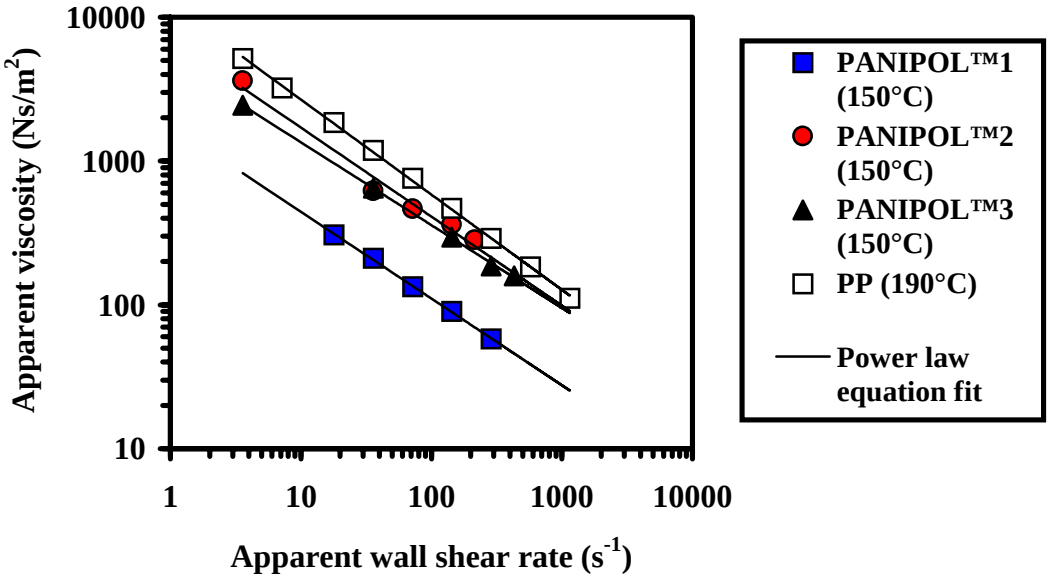

Figure 4.28. Variation of the apparent viscosity with respect to apparent wall shear rate for the PP and PANIPOL™ samples capillary extruded at 190 and 150°C, respectively.

Despite the presented results are from different experimental temperatures, fig. 4.28 indicates that the viscosities of the pellets of PANIPOL^{TM} extruded at a lower temperature, are yet of a lower magnitude than that of the PP extruded at a higher temperature. This suggests that the viscosity of any PANIPOL^{TM} sample would be of a considerably lower magnitude than that of the PP at comparable temperatures. Moreover, this also suggests that the ratio of the viscosity of any PANIPOL^{TM} sample to that of the PP, that is, p (already defined in section 2.6.1), would be even lower than that with respect to the viscosity of the SBS and LDPE, respectively.

Overall, the results suggest that, in principle, the three analysed polymer matrices could be suitable to be blended with the PANIPOL^{TM} samples. This is observed considering that the shear viscosity exhibited by these polymers is of a reasonably higher magnitude than that of the PANIPOL^{TM} samples, thus suggesting that these could act as carriers for the dispersed PANIPOL^{TM} phase, and hence promote the in-situ formation of polyaniline fibres in the blends. However, from the three analysed polymer matrices, it is believed that the SBS would produce better results. This is because, compared with the LDPE, the SBS displayed higher levels of viscosity, which would promote best the deformability of the dispersed conducting phase. With respect to the PP, a thermally produced blend of this polymer with any PANIPOL^{TM} sample would mean the exposure of the latter to temperature levels not lower than the melting point of PP (i.e., about 168°C). Furthermore, subjecting the resultant blend to a possibly further thermal process would result (as observed from the thermal analysis results) in the unavoidable loss of some of the additives originally present in the PANIPOL^{TM} samples. On the other hand, the PANIPOL^{TM} phase would be considerably fluid under these temperature conditions. Therefore, in the event that the conducting complex is deformed into fibres, their stability would be lower than that of the elongated domains that would be generated using LDPE or SBS. In consequence, this would increase the probability that the fibres break up into small droplets.

With respect to the PANIPOL^{TM} samples, it is believed that the three samples could be deformed into fibres following an in-situ deformation process since their viscosities were lower than those of the polymer matrices. However, the fact that PANIPOL^{TM} 2 proved to be the most viscous sample, suggests that its elongated domains would be the most stable and likely to maintain the desired morphology.

4.7 CONDUCTIVITY MEASUREMENTS.

The direct current (DC) electrical conductivity was evaluated at room temperature on the as-received cylindrical-shaped pellets of PANIPOL^{TM} 2 and on a selected extrudate of this sample. The main interest during the development of the present experiments was to measure the ability of the pellets of PANIPOL^{TM} to conduct electricity, especially through the bulk of the sample. Also, it was important to analyse how the ability of the electrical conduction would be affected if the sample was previously subjected to a processing method in which this would be exposed to the different processing parameters, for example shear stresses and temperature. Of main concern was also the implementation of a straightforward technique capable of yielding the more possible genuine results without altering, as much as possible, the microstructure of the sample. Of primordial importance when performing the electrical measurements is to choose the most suitable electrode system to ensure that the conduction of electricity through the sample could take place with the less possible level of disturbance. For this, the electrodes should be of a material that is readily applied, allows intimate contact with the specimen surface, and introduce no appreciable errors because of electrode resistance or contamination of the specimen. The electrode material should also be corrosion resistant under the conditions of test. The more common methods used for measuring the electrical conductivity of materials, the two- and four-probe techniques, generally involve the use of pressure contacts, silver paste and thread-cutting screws as electrodes (see for example references 176 to 179 and the references cited therein). However, none of those methods would suit our requirements considering the brittle nature of the materials. As explained before, the extrudates of the PANIPOL^{TM} pellets were very brittle and the pellets themselves showed a considerable degree of brittleness. Also, the dimensions of the specimens would not allow the application of a silver paste to the polished sample surfaces. Moreover, it is very likely that the polishing action would result in disintegration of the sample. Consequently, a technique was implemented by using mercury as electrical probes and a Keithley 614 electrometer for measuring the electrical resistance of the samples. For this, the electrometer employs the constant current technique [180] in which a voltage source within the instrument drives a constant current through the sample of unknown resistance. As the voltage developed across the sample is proportional to its resistance,

the instrument thus provides an output signal corresponding to the resistance of the sample under test. The constant current values generated by the instrument are dependent on the resistance range selected by the operator during the measurements. These values are presented in the appendix No. 2. Figure 4.29 shows the basic circuit configuration employed by the instrument during the resistance measurements.

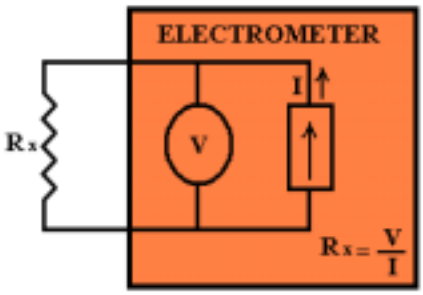

Figure 4.29. Diagram showing the basic circuit configuration [180] employed by the Keithley 614 electrometer during the resistance measurements. Rx = sample resistance, V = internal voltage source, I = current generated by the voltage source.

For the experiments, each sample was carefully enclosed in a soft temporary fastening resin and, to assure an effective contact with the probes, special care was taken in leaving both of its ends free of the resin. The sample so enclosed in the resin was inserted in the middle of a rectangular pool-like container (fig. 4.30). By doing this, the original container was thus divided into two cavities in which the liquid mercury would eventually be poured. The container was made of the same resin used for enclosing the samples.

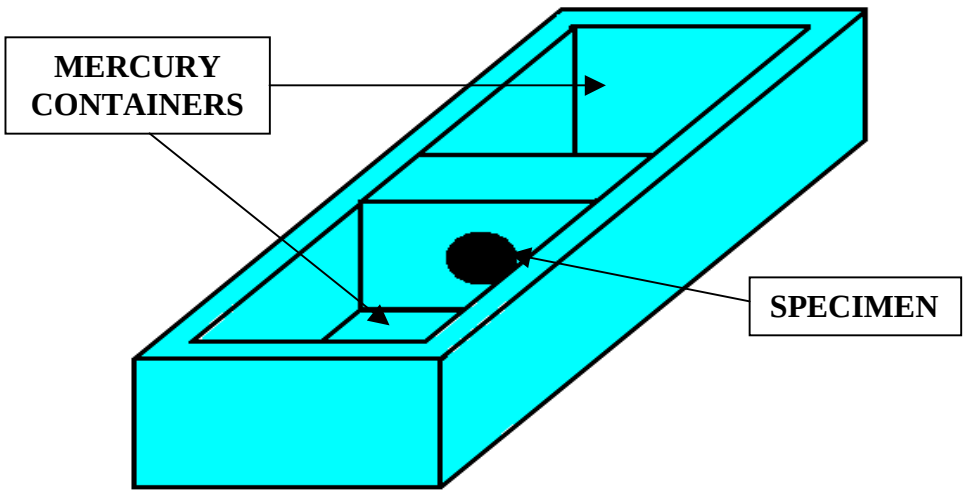

Figure 4.30. Diagram showing the manner in which the specimens were mounted for the electrical measurements.

To avoid the flow of the mercury between the containers, extra care was taken in ensuring that these were perfectly sealed. A very fine microspatula and a magnifying glass were used for aiding in the operations described above. Stainless steel needles of very low resistance, soldered to the electrometer input lead, were inserted into the lateral walls of the containers in which the liquid mercury was further poured. The arrangement described is depicted in figure 4.31. The dimensions of the specimens were measured by using a vernier. Accordingly, the tested pellets were about 3 mm in diameter and 2.7 mm in length. Selected extrudates obtained at 120°C and 1.25 mm/min (refer to section 4.6) were also tested. Their dimensions were about 1.60 mm in diameter and 4 mm in length.

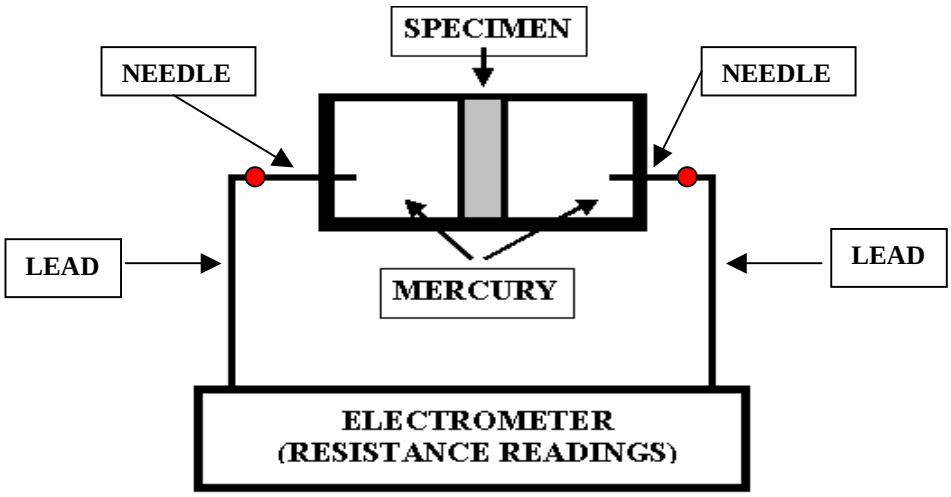

Figure 4.31. Arrangement used in the experiments performed for the volume conductivity evaluations.

The electrical resistance readings were performed using the lowest possible resistance range and these were taken after 5 min of sample electrification to allow the system to stabilise. After taking the readings, the mercury was recovered and poured into its corresponding storing flask. In all the experiments, a syringe and disposable micropipettes were used for handling the mercury. After the end of each experiment, the sample embedded in the resin together with the resin-made containers were safely disposed of in a flask containing a water bath. Five specimens from each type of material were tested. Assuming that the resistance readings were performed at an ohmic regime [179,181] and that the specimens were perfect cylinders, the volume

conductivity was then evaluated in accordance with the dimensions depicted in fig. 4.32 and using the following equation:

$$\sigma = \frac{l}{AR} = \frac{4l}{\pi d^2 R} \text{ .....Eq. 4.5,}$$

where:

σ = specimen volume conductivity,

l = specimen length,

A = specimen cross sectional area,

R = measured volume resistance, and

d = specimen diameter.

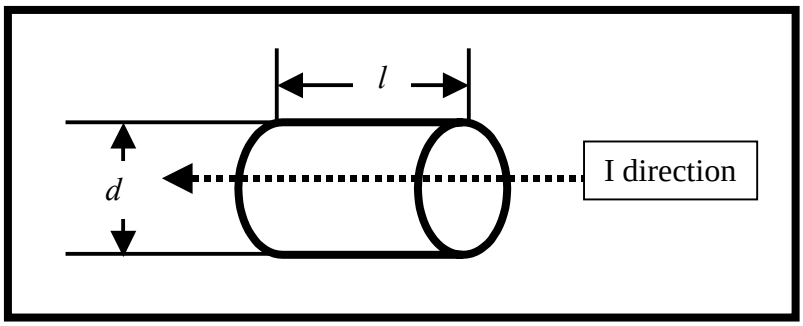

Figure 4.32. Diagram exemplifying the specimen dimensions.
I = current, l = specimen length, d = specimen diameter.

The volume conductivity of the pellets of PANIPOL™ 2 and their extrudates are presented in Table 4.5.

Table 4.5. Results from the volume conductivity measurements on PANIPOL™ 2.

PELLETS				
Sample	***d* (mm)**	***l* (mm)**	***R* (kΩ)**	**σ (S/cm)**
1	3.14	2.71	0.858	4.08×10^{-3}
2	2.95	2.63	0.911	4.22×10^{-3}
3	2.87	2.79	3.130	1.38×10^{-3}
4	2.98	2.83	2.270	1.79×10^{-3}
5	2.91	2.64	2.890	1.37×10^{-3}
Average				**2.6×10^{-3}**
Standard deviation				**1.5×10^{-3}**

Table 4.5 (Continued).

PELLETS CAPILLARY EXTRUDED AT 120°C AND 1.25 mm/min				
Sample	***d* (mm)**	***l* (mm)**	***R* (kΩ)**	**σ (S/cm)**
1	1.62	2.87	6.18	2.25×10^{-3}
2	1.66	4.16	3.67	5.24×10^{-3}
3	1.62	3.26	7.86	2.01×10^{-3}
4	1.63	4.28	9.23	2.22×10^{-3}
5	1.80	4.58	3.20	5.63×10^{-3}
Average				**3.5×10^{-3}**
Standard deviation				**1.8×10^{-3}**

It was observed that, during the measurements of the electrical resistance, the values displayed by the measuring instrument rapidly increased as soon as the sample was electrified by the electrometer. This was observed in the majority of the experiments. However, the resistance readings stabilised after about 4-6 minutes of sample electrification, thus indicating that the current flow driven by the electrometer through the bulk of the sample was also stable. With respect to this, it has been reported [182] that the response of a polymer to an applied current may be delayed due to a number of factors including the interaction between the polymer chains, the presence within the chain of specific molecular groupings, and effects related to interactions within the specific atoms themselves. Therefore, this can be a possible explanation regarding the observed lag in the stabilisation of the resistance readings. As indicated before, all the readings were taken after 5 min of sample electrification and, as observed in Table 4.5, the calculated conductivity values show a considerable level of consistency.

From the results presented in Table 4.5, it can be seen that the extruded material exhibited a slightly higher level of conductivity than that shown in the pellets. This may be due to the action of elongational flows, occurring during the extrusion process, on the macromolecules of PANI. This would promote the orientation and alignment of these in the direction of the current flow during the experiments and the consequent reduction on the resistance levels observed. From the results, it can be seen that the obtained overall average value of about 3×10^{-3} S/cm compare well with the value of 10^{-4} S/cm reported by Neste Oy Chemicals [71].

4.8 MORPHOLOGICAL ANALYSIS.

This analysis was performed with the purpose of obtaining information, at a microscopic scale, on the form and structure of the pellets of PANIPOL^{TM}. This information, together with the information gained from the previous characterisation analyses (specially those concerning gravimetry and IR spectroscopy) would broaden the knowledge about the nature of the samples' components, providing at the same time with some information about their microstructure. As mentioned before, the interpretation of the results is based on the information provided by the manufacturer and the experimental results reported in the literature related to systems apparently similar to the present one. For the analysis, optical and scanning electron microscopy techniques were followed. These are detailed in the following sections.

4.8.1 OPTICAL MICROSCOPY.

The morphology of the pellets of PANIPOL^{TM} 2 was initially examined using a Reichert Microstar 110 optical microscope. For this, few of the as-received pellets were pulverised with a pestle and mortar. A small amount of the powder was mounted on a glass slide and the microscopic analysis was performed using transmitted and incident light respectively.

Figure 4.33 presents the morphology found in different granules of the powder pellets. It can be observed that some areas of the photographs are blurred indicating that those sections in the granules were out of focus during the analysis. This is the result of the irregular thickness of the granules as no special technique was followed in the preparation of the sample other than mere pulverisation of the pellets. However, from the micrographs, spherical features can be seen dispersed all over the bulk of the granules. These spherical features are more evident in the samples analysed under incident light. For example, note the features reflecting the light in the encircled area shown in fig. 4.33b. The granules analysed under transmitted light (fig. 4.33d) do not show the above mentioned spherical features very clearly as the sample was too thick as to allow the light to pass through it. However, some sections of the analysed granules do show some features that can be associated with the aforementioned globular features. For instance, observe the areas encircled in fig. 4.33d. These sections of the sample are

abundant in spherical features. This can be confirmed by observation of fig. 4.33c, which is a micrograph of the same granule but analysed under incident light.

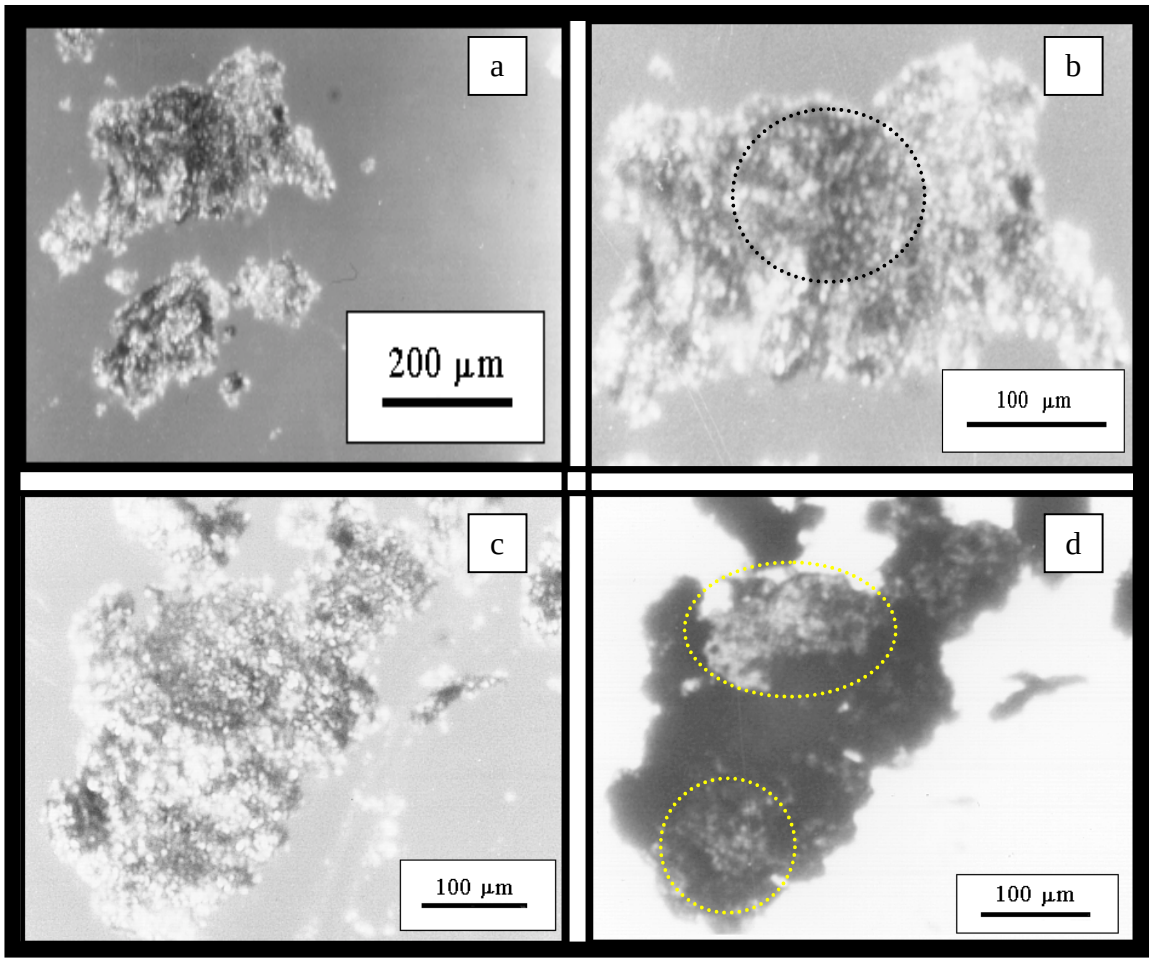

Figure 4.33. Optical micrographs of granules of the powdered PANIPOL™ 2. Figures (a), (b) and (c): sample analysed under incident light. Figure (d): the same granule as in fig. (c) but analysed under transmitted light. Figure (b) is a magnification of fig. (a).

As can be seen in fig. 4.33c the same sections encircled in fig. 4.33d contain a great number of globular features reflecting the light. These observations seem to suggest that the observed globular features are bound together by a different material, thus indicating that the morphology of the pellets of PANIPOL™ 2 consists of at least two different phases, one in the form of spherical particles and another one serving as a dispersing medium. Through this analysis it is not possible to have a clear estimate about the size of the observed particles as the photographs were not taken at high enough magnifications. This will be indicated better in the section concerned with the

scanning electron microscopy analysis. However it can be seen that the particle diameters should be about a few microns.

The morphology presented in fig. 4.33d resembles the ones observed by Lux et al. [54,55] for heavily doped polyaniline with hypochloric acid. These researchers found that their powdered samples consisted of spherical particles of conducting polyaniline incorporated into a less dense matrix. Similar morphologies have also been observed by other researchers for conducting polyaniline prepared by means of different routes, namely conventional chemical [56,63] and dispersion [10,61,62] polymerisation, respectively. It is however, worth pointing out that the diameters reported for the polyaniline particles in the above works were all within a nanometric scale, which differ considerable with the size of the particles observed in the present samples. However, as is also mentioned in the references cited above, the size of the conducting domains depends on the synthesis route of the polymer, and what is more, diameters of about 20-50 μm have also been reported [20,66]. Consequently, it is believed that the observed spherical features in the powdered sample in question correspond to the conducting polyaniline particles dispersed in a continuous phase.

4.8.2 SCANNING ELECTRON MICROSCOPY.

Scanning electron microscopy (SEM) analysis was performed on an as-received pellet of PANIPOL^{TM} 2 as well as on the powdered pellet. The analyses were performed with a JEOL JXA-840-A electron probe microanalyzer at 10 kV. For the analysis, the samples were previously gold coated for 4 min in an E5000 (Polaron Equipment Limited) SEM coating unit.

The morphology of the pellets is presented in figure 4.34. Figure 4.34a corresponds to the cross sectional surface of the pellet while figs. 4.34b to 4.34d correspond to a granule of the pulverised pellets observed at different magnifications. As can be seen, these figures show the presence of globular features in the analysed samples. Again, these globular features are believed to be the conducting particles of polyaniline embedded in a continuous phase. These SEM micrographs, in contrast to the optical ones, are more suitable for estimating the size of the polyaniline particles, which are about 7 μm in diameter or of a smaller size.

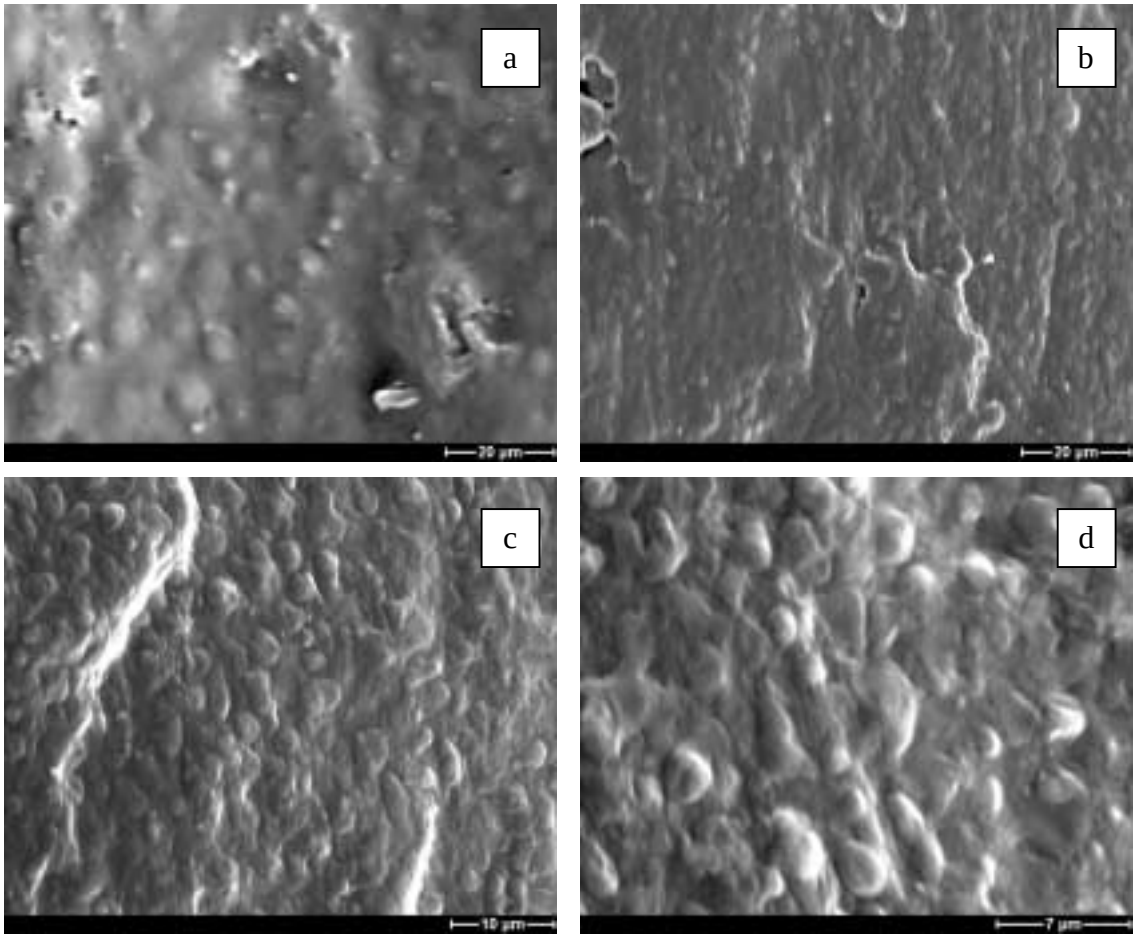

Figure 4.34. SEM micrographs of PANIPOL^{TM} 2. Fig. (a): cross sectional surface of the as-received cylindrical pellet. Figs. (b), (c) and (d): powdered pellet at different magnifications.

It is interesting to notice that the features observed on the cross sectional surface of the pellet (fig. 4.34a) seem to reveal well-formed spheres. This differs from the particles observed in the granule of the pulverised pellet that show irregular shapes (figs. 4.34b to 4.34d). Moreover, most of the particles shown in the cross section of the pellet are of a larger size than those observed in the pulverised pellet (fig. 4.34b). The smaller size of the particles observed in fig. 4.34b might be due to the effect of the crushing process to which the pellets were subjected during their pulverisation, thus resulting in the break up of the original particles into particles of smaller size. Figures 4.34b to 4.34d also reveal that the analysed granules of the pellet are composed of densely packed conducting polyaniline particles.

The knowledge of the preparation route followed during the production of the pellets is very limited as the manufacturer provided no specific information on the

subject. However, Virtanen and co-workers [28], researchers from Neste Oy Chemicals, the company supplying the pellets, point out that fusible PANIPOL^{TM} compositions are produced by a reactive extrusion process in which the polyaniline salt, the plasticizer, and other optional additives are fed into a twin-screw extruder to produce further solidified strands of the conductive material which are subsequently cooled, pelletised and packaged. Consequently, it is assumed that this was the production method employed for the manufacture of the pellets subject of this study. Furthermore, it is believed that the morphology observed in the SEM micrographs originated as a result of the clustering of aggregates (formed of primary doped polyaniline nanoparticles) into the globular shaped agglomerates observed in the photographs. This type of morphology, with the characteristics of a colloidal system [183], has been reported [20] for polyaniline-DBSA dispersions in which an excess of DBSA forms micellar structures and also acts as a surfactant, which also stabilises the dispersion. In morphologies like this (fig. 4.35), the hydrophobic tails (i.e., the alkyl benzene moiety) of free and bonded DBSA molecules are arranged in a way that they all turn to each other, while the hydrophilic groups (i.e., the sulphonic moiety) of the free DBSA turn to the aqueous phase.

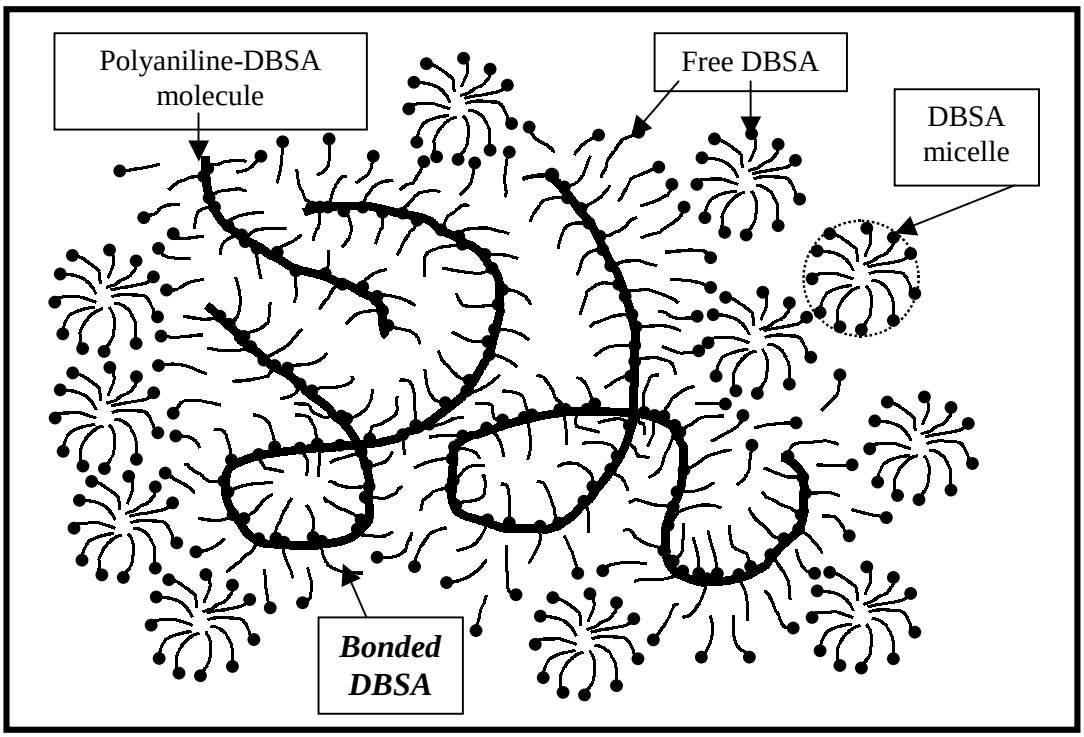

Figure 4.35. A schematic model of an aqueous dispersion of polyaniline with DBSA [20].

As mentioned before, it is difficult to be certain whether the system previously described fully resembles the one investigated in this work. However, they are compared based on the fact that it has been identified the surfactant character of the doping agent (DBSA) and plasticizer (the Zn salt of DBS) used in the production of the pellets. Furthermore, it is suspected that some DBSA may be present in excess in the pellets. Also it may be possible that another compound, derived from the DBSA, was used as another additive (perhaps as a compatibility agent) for the production of the material. Therefore, it is likely that the hydrophilic (i.e., the $–SO_3–$ groups) and hydrophobic (i.e., the alkyl-phenyl group) moieties of the DBSA, simultaneously form hydrogen bonds and ring-ring interactions with, respectively, the –NH– groups and the phenyl rings of the electrically conducting polyaniline (fig. 4.36). This has been reported by Ikkala et al. [184] (in a patent assigned to Neste Oy Chemicals) to occur in conducting compositions of polyaniline.

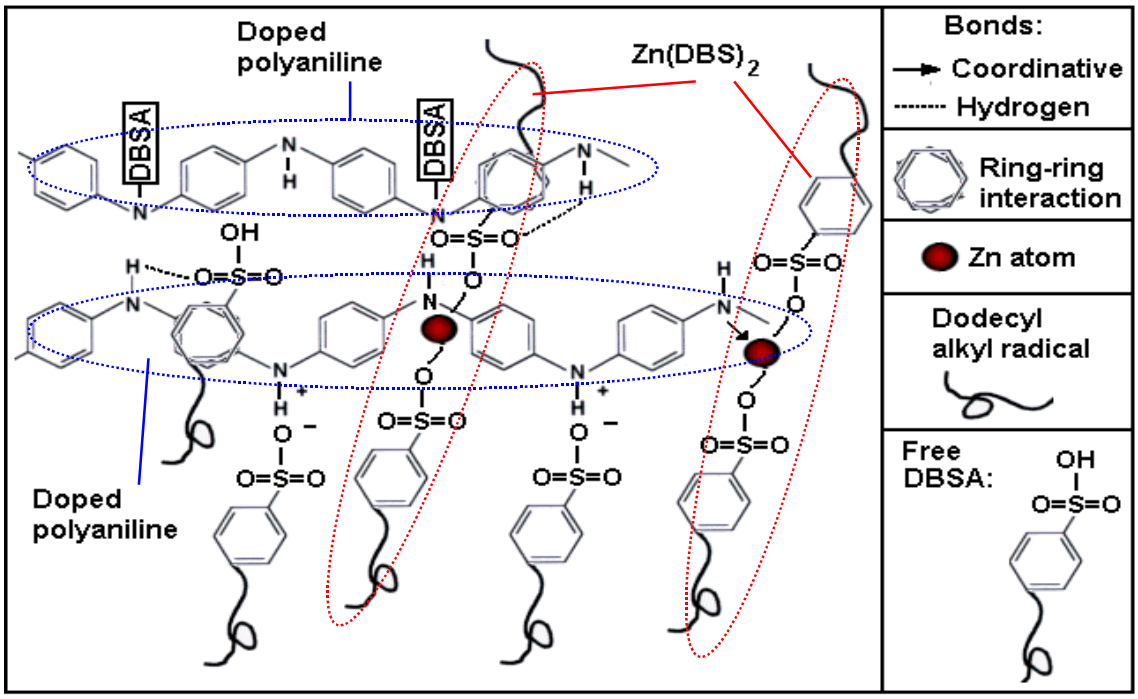

Figure 4.36. Schematic representation of the suggested molecular interactions in the pellets of PANIPOL^{TM}.

The presence of DBSA in excess (or another derived compound) in the pellets may promote the formation of a solid dispersion of conducting polyaniline particles with the structured morphology observed (for instance see fig. 4.34b). The aforementioned hydrogen bonds and ring-ring interactions would form an infinite

network that stabilises the conducting dispersion. On the other hand, as also reported [28], the metal atom from the Zn salt of DBS would form coordinative bonds [185] with the nitrogen atoms of the doped polyaniline chains (fig. 4.36). Again, it is thus possible that the hydrophilic and hydrophobic moieties of the dodecylbenzene sulphonate ion (DBS) would also form hydrogen bonds and ring-ring interactions with the polyaniline molecules, thus enhancing the formation of the observed morphology and the stabilisation of the dispersion.

4.9 CONCLUSIONS.

The results from the X-ray diffraction experiments revealed that the level of crystallinity detected in the PANIPOL^{TM} samples was relatively low. The presence of the element Zn in the pellets was also confirmed through this analysis.

The gravimetric analysis confirmed the amount of the conducting polyaniline salt in the pellets of PANIPOL^{TM} (that is, about 25 wt. %). This analysis also aided in establishing an initial hypothesis about the use of DBSA and a Zn salt of DBS in the manufacture of the pellets.

The concept about the use of DBSA and a Zn salt of DBS as the doping and Zn compounds, respectively, was reinforced by the results yielded from the FTIR analysis.

The thermal limitations of the PANIPOL^{TM} samples were established through TGA and DSC analyses. These analyses confirmed that the samples could be safely processed up to a maximum temperature of about 250°C without exposing them to severe degradation and loss of their electrically conductive characteristics. However, the DSC analysis suggested an inhomogeneous distribution of the components (especially those of additive nature) in the samples during the manufacturing process. Also, it was found that the pellets might not maintain their intrinsic properties even when exposed to the so-called safe processing range of temperatures, thus implying that there are limitations regarding their reprocessability.

The rheometry analysis performed on the PANIPOL^{TM} samples evinced an erratic behaviour of pressure versus time during the experiments. This behaviour, attributed to

the inhomogeneous character of the samples, is believed to be associated with the high degree of brittleness and poor surface finish observed in the extrudates. It was observed, however, that the degree of brittleness was most evident at lower extrusion speeds and at higher temperature levels. The analysis also suggested that, compared with the LDPE and PP, the SBS seemed to be the most suitable material to be blended with the PANIPOL^{TM} samples as this would best favour the in-situ formation of polyaniline fibres in the blends. This is because the SBS possesses the required level of viscosity, together with a suitable processing temperature for processing the conductive complex without risking its electro-conductive performance. In the same way, the analysis suggested that using PANIPOL^{TM} 2 would produce better results as this sample proved to be the most viscous of the three PANIPOL^{TM} samples, thus suggesting that in a blend, with for example SBS, it would possess better stability, which would aid in maintaining the desired morphology.

The level of electrical conductivity measured in the PANIPOL^{TM} extrudates was slightly higher than that in the pellets. This may be due to the action of elongational flows occurring at the entrance of the capillary die during the extrusion process, which in turn would promote the orientation and alignment of the polyaniline macromolecules in the direction of the current flow. The obtained overall average value of 3.03×10^{-3} S/cm compares well with the value of 10^{-4} S/cm reported by the company supplying the material.

The morphological analysis performed on the pellets of PANIPOL^{TM} showed the presence of spherical features surrounded by a continuous phase. These features, which are about 7 μm in diameter (or of a smaller size), are believed to be the particles of the polyaniline salt. Furthermore, it is believed that the morphology observed was originated as a result of the clustering of aggregates (formed of primary doped polyaniline nanoparticles) into globular shaped agglomerates. It is likely that the hydrophilic and hydrophobic moieties of the DBSA and its derived Zn salt simultaneously form hydrogen bonds and ring-ring interactions with, respectively, the –NH– groups and the phenyl rings of the electrically conducting polyaniline. The possibly presence of DBSA in excess (or another compound derived from this) in the pellets may enhance the formation of a solid dispersion of conducting polyaniline particles stabilised by the aforementioned hydrogen bonds and ring-ring interactions.